Study of the C.O.P. of steam jet refrigeration unit as compared to vapor compression unit

A Thesis

Submitted to Al-Nahrain University College of Engineering in Partial Fulfillment of The Requirements For The Degree of Master of Science in Mechanical Engineering

By

Ahmed Jameel Hamod Al-Zaidy

(B.Sc.2001)

Safar 1425
April 2004

Certification

I certify that the preparation of this thesis entitled "Study of the C.O.P. of steam jet refrigeration unite as compared to Absorption system", was prepared by Engineer Ahmed Jameel Hamod Al Zaidy, under my supervision at Al Nahrain University in partial fulfillment of the requirements for the degree of Master of Science in Mechanical Engineering.

Signature:
Name: Dr. Adnan A. Al-Qalamchi
Date: / /2004

Signature:
Name:
Head of Department
Date: / /2004

We certify that we have read this dissertation entitled “Study of the C.O.P. of steam jet refrigeration unite as compared to Absorption system”, and as an examining committee, examined the student in it’s contents and that in our opinion it meets the standard of a dissertation for the degree of Master of Science in Mechanical Engineering.

Signature:
Name: Dr.Adnan A.Al-Qalamchi
(Supervisor)
Date: / /2004

Signature:
Name:
(Chairman)
Date: / /2004

Signature:
Name:
(Member)
Date: / /2004

Signature:
Name:
(Member)
Date: / /2004

Approved by the Dean of the College of Engineering:

Signature:
Name: Prof.Dr.Fuzzy
(Dean of Engineering College) Date:
/ /2004

Acknowledgment

In the name of ALLAH, The gracious the all merciful

Praise to ALLAH for providing me the willingness and strength to accomplish this work.

It is pleasure to record my indebtedness to my supervisor Dr.Adnan Al-Qalamchi for his help during this work and for the chance he gave me to enter to the world of Study of the C.O.P. of steam jet refrigeration unite as compared to Absorption system.

Very special thanks are due to my father for his help and encouragement.

Special words of thanks and deepest gratitude are presented to my mother for her patience and compassion during this work.

My thanks also extended to the head and staff members of the department of Mechanical engineering for all the facilities offered.

Thanks are expressed to all my friends especially to Engineer Ali Hussain, Saif, Fady, Sinan, Husam.

Finally, special thanks are devoted to my family for their care during this work.

Ahmed Jameel Hamod Al-Zaidy

April 2004

Abstract

The present study has been carried out to investigate the performance of the steam jet refrigeration system at various operating conditions, and to compare the C.O.P. results with that of Absorption system.

The study includes design analyses of the ejector performance. The performance enhancement options and desired ejector geometry are also examined. The coefficients of performance for a simple ejector was found to range between (0.5 to 1.168) for the cooling mode and (1.5 to 2.168) for the heating mode at a sample operating condition in which the boiler temperature varies between (100-150^{o}C), Condenser temperature between (45-60^{o}C), and evaporator temperature between (3-9^{o}C).

Theoretical comparison of the C.O.P. was made between the Steam jet refrigeration system and Absorption system. The results show that the C.O.P. of the two systems decreases with condenser temperature rise, but the C.O.P. of the former system is larger than that of the second, and the C.O.P. of the former was found to decrease with evaporating temperature rise, while the C.O.P. of the second system increase.

For the steam jet refrigeration system it was found that the secondary vapor mass flow rate increases with increasing boiler temperature and ejector throat area, and it decrease when condensing and evaporating temperatures increases.

The study revealed that with larger ejector throat area the secondary vapor mass flow rate becomes higher giving rise to system capacity at a given set of conditions.

Contents

Abstract	I
Contents	II
Nomenclatures	V
Chapter one: Introduction	1
Chapter two: Literature survey	5
Chapter three: Theoretical Analysis	19
3.1 Introduction	19
3.2 Description of the model	20
3.2.1 Evaporator	20
3.2.2 Condenser	23
3.2.3 Boiler	24
3.2.4 Steam-jet ejector	25
3.3 General Assumptions	27
3.4 Design considerations	27
3.4.1 Nozzle	28
3.4.2 Ejector suction opening and suction chamber	29
3.4.3 Mixing section	30
3.4.4Constant area section	30
3.4.5 Subsonic diffuser	31
3.5 Controls	32
3.6 Analysis of system components	33
3.6.1Ejector efficiency	33

3.6.2 Optimum ejector analysis 35
3.6.3 Ideal cycle performance 42
3.6.4 Non-ideal cycle calculations 43

Chapter four: Results and Discussion 47
4.1 The variation of the system characteristics with boiler temperature
with different throat areas. 47
4.1.1 Effect of boiler temperature on primary
vapor flow rate. 47
4.1.2 Effect of the boiler temperature on secondary
vapor flow rate. 49
4.1.3 Effect of the boiler temperature on the
cooling Coefficient of performance. 51
4.1.4 Effect of the boiler temperature on the
system capacity . 53
4.1.5 Effect of the boiler temperature on the
heating Coefficient of performance . 54
4.2 The variation of the system characteristics
with condenser temperature at different throat areas. 56
4.2.1 Effect of the condenser temperature on
the evaporator mass flow rate. 56
4.2.2 Effect of the condenser temperature on
the cooling coefficient of performance. 58
4.2.3 Effect of the condenser temperature
on the heating Coefficient of performance. 60
4.2.4 Effect of the condenser temperature on
the system capacity. 61
4.3 The variation of the system characteristics

with evaporator temperature for the variation throat areas. 63

4.3.1 Effect of the evaporator temperature on the evaporator flow rate. 63

4.3.2 Effect of the evaporator temperature on the cooling Coefficient of performance. 65

4.4 Comparison of the Coefficients of performance between the Steam jet refrigeration system and the Absorption system with condenser temperature. 66

4.5 Comparison of the Coefficients of performance between the Steam jet refrigeration system and the Absorption system with evaporator temperature. 67

Chapter five: Conclusions and Recommendations for future work

5.1 Conclusions 69

5.2 Recommendations for future work 70

References 71

Appendix A: Table of results A-1

Appendix B: Sequence of steps for the Mat lab program B-1

Appendix C: Absorption system C-1

Nomenclature

Symbol	***Definition***	***Units***
A	Area	m^2
A_{th}	Throat area	m^2
A_2	Diffuser throat area	m^2
a	Velocity of sound	m/s
$C.O.P._c$	Cooling Coefficient of performance	
$C.O.P._h$	Heating Coefficient of performance	
C_p	Specific heat at constant pressure	$kJ/kg.^oC$
E	Total energy	kJ
e	Total energy per unit mass	kJ/kg
g	Acceleration of gravity	m/s^2
h	Enthalpy	kJ/kg
h_o	Enthalpy of the Saturation motive flow	kJ/kg
h_t	Stagnation enthalpy	kJ/kg
h_1	Exit nozzle enthalpy	kJ/kg
h_{1s}	Isentropic Exit nozzle enthalpy	kJ/kg
h_2	Enthalpy at diffuser throat area	kJ/kg
h_3	Enthalpy of Saturation steam at Condenser temperature	kJ/kg
$h_{3'}$	Ideal condenser enthalpy	kJ/kg

h_4	Enthalpy of Saturation steam Evaporator	kJ/kg
h_5	Enthalpy of the Saturation liquid at condenser temperature	kJ/kg
h_7	Enthalpy of the Saturation liquid at evaporator temperature	kJ/kg
k	Isentropic exponent	
$K.E.$	Kinetic energy	kJ
M	Mach number	
M_2	Mach number at Diffuser throat area	
$\dot{m}$	Mass flow rate	kg/s
$\dot{m}_o$	Motive Mass flow rate	kg/s
$\dot{m}_4$	Secondary Mass flow rate	kg/s
P	Pressure	Pa
$P.E.$	Potential energy	Pa
P_b	Saturation Boiler pressure	Pa
P_e, P_{ev}, P_4	Saturation Evaporator pressure	Pa
P_t	Stagnation pressure	Pa
P_1	Exit nozzle pressure	Pa
P_2	Pressure at Diffuser throat area	Pa
P_3	Saturation condenser pressure	Pa
Q	Capacity	kJ
R	Gas constant	$J/kg.K$
s_o	Boiler entropy	$J/kg.K$
s_3	Condenser entropy	$J/kg.K$

s_4	Evaporator entropy	$J/kg.K$
T	Temperature	^oC
T_b	Saturation Boiler temperature	^oC
T_c , T_{con}	Saturation Condenser temperature	^oC
T_e , T_{ev}	Saturation Evaporator temperature	^oC
T_t	Stagnation temperature	^oC
T_1	Exit nozzle temperature	^oC
T_2	Temperature at Diffuser throat area	^oC
$T_{3'}$	Ideal condenser temperature	^oC
t	Time	s
U	Internal energy	kJ
u	Internal energy per unit mass	kJ/kg
V	Velocity	m/s
V_2	Fluid velocity at diffuser throat area	m/s
v_2	Specific volume at diffuser throat area	m^3/kg
W	Work	kJ
z	Head	m
ρ	Density	kg/m^3
η_d	Diffuser efficiency	
η_E	Ejector efficiency	
η_n	Nozzle efficiency	
$\forall$	Volume	m^3

Chapter one

Introduction

Air-conditioning and refrigeration equipment play very important role in modern human life. The utilization of these equipment in homes, buildings, vehicles, and industries provides for living comfort and necessary means for industrial production.

However, the large amount of energy consumed by this equipment consequently becomes a serious problem to be solved. Thus it is desirable to seek a new technique, which can effectively and economically use heat such as oil and coal as an energy source to directly power airconditioning and refrigeration system and can operate at relatively low temperature, and has very stable performance characteristics. Recent investigations have shown that it appears to be a favored choice for this purpose. The steam or vapor jet refrigerant system is one of such systems.

For many years ejectors have been used extensively in power generating plants and have found wide application in the chemical industries. In power plant practice they are used principally in exhausting air from condensers and in priming pumps. In the chemical industries they are utilized in vacuum evaporation, filtration, compressing air for agitation, and in pumping of liquid and gases. During the early 1930's, ejectors had been used in steam jet refrigeration units for air conditioning large buildings, and for industrial uses such as the chilling of water to moderate temperatures in process industries. [1]

The design of jet refrigeration system is similar to that of conventional vapor-compression system except that the mechanical compressor is replaced by a thermal compressor, which is usually, called an “ejector”.

The jet refrigeration system consists of four basic components: -

1- An ejector

2- An evaporator,

3- A generator,

4- A condenser. Figure (1-1) shows such a system

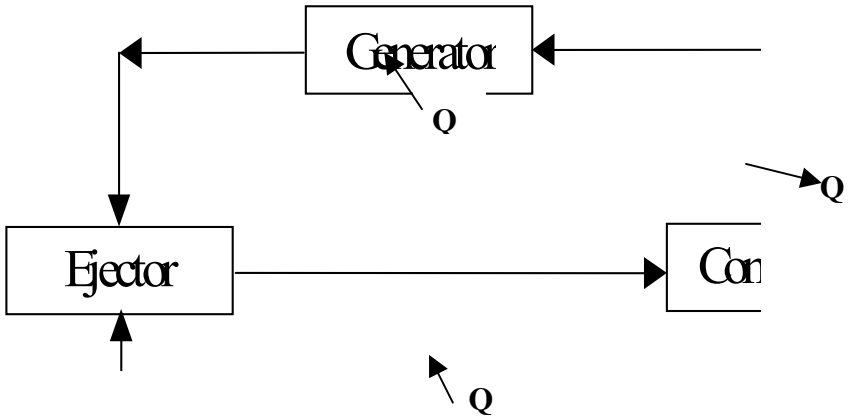

Figure (1-1) Schematic diagram of jet refrigeration system.

The ejector is the heart of the jet refrigeration system. The characteristics of this component have a major effect on the operating cost of the system, and the size of both condenser and generator. Ejector is a pump having no moving parts and utilizing fluids in motion under controlled condition. Specifically, motive power is provided by a high pressure stream of fluid directed through a nozzle designed to produce the highest possible velocity.

The resultant jet of high-velocity fluid creates a low-pressure area in mixing chamber causing the suction fluid to flow into this chamber. Ideally, there is an exchange of momentum at this point producing a uniformly mixed stream traveling at a velocity intermediate to the motive and suction velocity. The diffuser is shaped to reduce the velocity gradually and convert the energy to pressure at the discharge with as little loss as possible. The three basic parts of any ejector are the nozzle, the mixing section, and the diffuser.

Ejectors may be classified on the basis of the conditions maintained in the mixing section. It is customary in the design of ejectors to assume either that:

- Mixing occurs at constant area with rising static pressure.
- Mixing occurs at constant static pressure in a converging section.

Generally, experience indicates the design based on the second assumption is substantially correct and if any slight increase in the static pressure results from mixing, the ejector performance will be better by the amount of this increase [2]. In this study the second assumption is considered.

Also, the analytical results indicate that constant-pressure mixing yields results superior to those obtained with constant-area mixing [2].

The evaporator is usually a large volume vessel, which must provide a large water surface area for efficient evaporative cooling action. Water sprays and cascading water in sheets are two common means of maximizing water surface.

The steam generator can provide the primary or motive steam that is needed to drive the system, i.e. providing the pressure, temperature and flow rate of the motive steam.

The condenser can be one of three basic types, a conventional surface condenser, an evaporative condenser and a barometric condenser.

As heat is added to the generator, the steam at fairly high temperature and pressure called primary or actuating steam is evolved and enters the ejector. By expansion through the nozzle inside the ejector, supersonic flow at low pressure is formed at the exit of the nozzle and has the secondary vapor entrained from the evaporator. The primary and the secondary vapors then mix with each other at the mixing section and enter the constant-area. An aerodynamic shock is induced to create a major compression effect.

Further compression of the mixture to the back pressure of the ejector can be achieved as it passes through the subsonic diffuser section. By this process in the ejector, the refrigerant vapor, which acts as the secondary vapor, is compressed aerodynamically from the lower pressure at the evaporator to the higher pressure at the condenser.

The inflow of the internal energy associated with the primary vapor serves as the energy input required for the compression operation. To obtain a cooling effect, part of the refrigerant condensate in the condenser is allowed to expand in the evaporator to absorb heat from the environment. The rest is recirculated to the generator by a liquid circulation pump to complete a cycle. [3]

In Iraq the heat energy is available in large amount and cheap cost, in time that the electric energy is expensive and not continuously available when needed. Therefore the use of airconditioning equipment, which depends directly on, the heat energy is important and can over come troubles resulting from electrical energy dependence. The heat energy depending system is the steam jet refrigeration system.

The performance of jet refrigeration system can be accurately calculated by use of the method of system analysis only when the performance characteristics of each component in the system are all clearly

understood. The coefficient of performance of the system is compared with an equivalent system like Absorption system.

Chapter two
Literature survey

The literature survey considered in this chapter shall cover works obtained on the design and performance of steam jet refrigeration system and the ejector.

A one-dimensional analysis of the mixing of two gas streams involving the application of the equations of continuity, momentum, and energy to the design of ejector was investigated by Flugel [3]. The mixing at constant area and at constant pressure was considered, but the published results of his calculations were meager.

Keenan and Neumann [4] applied the same method of analysis to ejectors with large ratios of mixing-tube area to the nozzle throat area and relatively small ratios of nozzle-inlet pressure to suction pressure. The object of their investigation, was to select the simple form of ejector which would perform in useful fashion, to analyze its performance as nearly independently of data on ejectors as possible, to compare the actual performance with that predicted analytically, and not to devise a new type of ejector. The results showed that:

1. When the ejector is serving as a blower, constant-area mixing is better than constant-pressure mixing because it gives higher flow ratio as shown in fig (2-1), except for area ratio less than 10
2. Experiments on the simple ejector showed that:
    i) The best position of the exit of the nozzle is only a short distance upstream from the throat of the diffuser.
    ii) The best length of the mixing tube is slightly greater than 7 diameter.

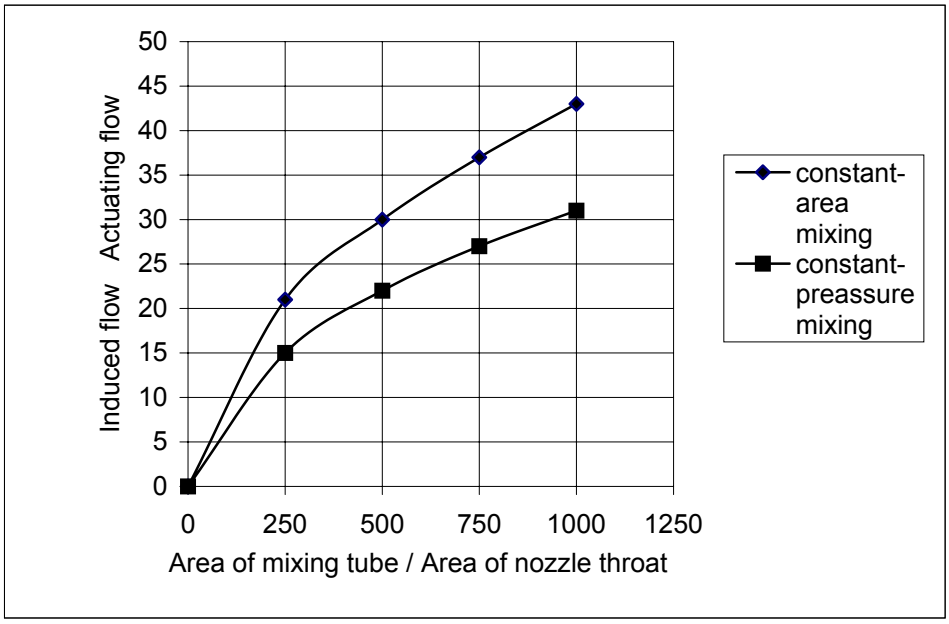

Fig (2-1) Performance of ejector

The flow ratio of induced-to-actuating fluid increases rapidly with the ratio of mixing-tube area to nozzle-throat area, and decreases with increase in the ratio of supply pressure to suction pressure, as shown in fig. (2-2).

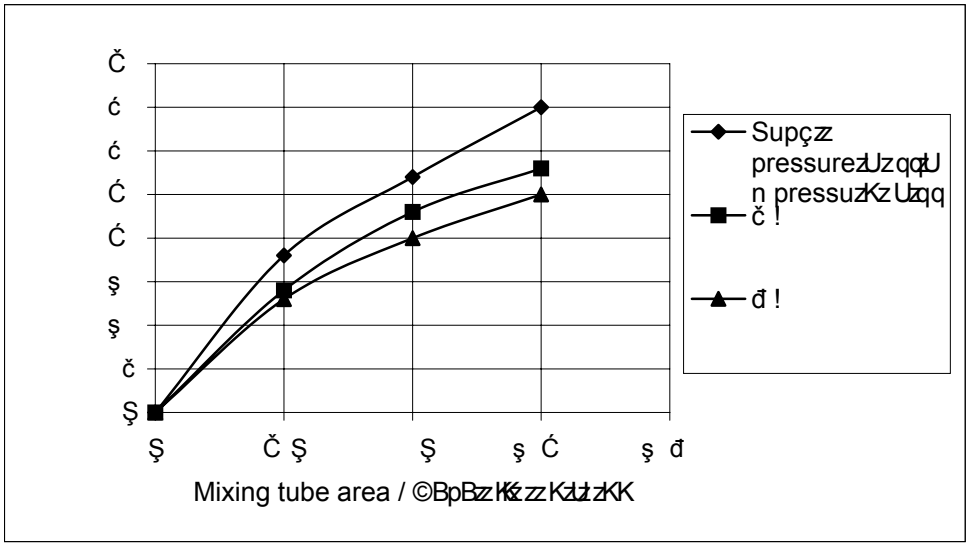

Fig (2-2) Flow ratio to Area ratio

Elrod [5] extended an ejector theory, which has previously been confirmed by the experiments of others. A new theoretical criterion of ejector performance and a new equation for ejector design included a calculation of optimum area ratios and optimum flow ratios were derived.

The optimum area ratio was devised by maximizing the induced mass flow subject to equations of conservation of mass, energy and momentum in the actuating nozzle, mixing tube and diffuser, which yield the following equation:

$$M_2^2\left[1-(1-\eta_d)\frac{T_2}{T_3}\left\{\left(\frac{d(\ln T_2/v_2)}{d(\ln v_2)}\right)+\frac{K_2}{1-P_o/P_2}\right\}\right]=1$$

Where:

M_2 = Mach number at inlet of the subsonic diffuser.

η_d =Diffuser efficiency.

T_2 = Temperature at inlet of the subsonic diffuser, K

T_3 = Temperature at exit of the subsonic diffuser obtained with isentropic compression, K

v_2 = Specific volume at inlet of the subsonic diffuser, (m^2/kg)

K= Specific heat ratio at the subsonic diffuser.

P_o/P_2 = Ratio of suction pressure to diffuser inlet pressure.

This equation was then combined with the equation of conservation of momentum in the mixing tube to produce,

$$a_2 = \frac{m_1 v_1 / g}{P_2\left[\frac{k_2 M_2^2 + 1}{P_3/P_2} - P_o/P_3\right]}$$

Where:

a_2 = Cross-section area at inlet of the subsonic diffuser, m^2

m_1 = Mass flow rates of the actuating fluid, kg/s

v_1 = Actuating velocity at the nozzle, m/s

P_3/P_2 = Ratio of pressure at the diffuser exit to pressure at inlet of the diffuser.

P_o/P_3 = Ratio of suction pressure to diffuser exit pressure.

From which the value $\frac{k_2 M_2^2 + 1}{P_3/P_2}$ is a function of (P_o/P_3), which is tabulated by Elrod [5] and plotted by Chem [6], as shown in (fig. (2-3) A and

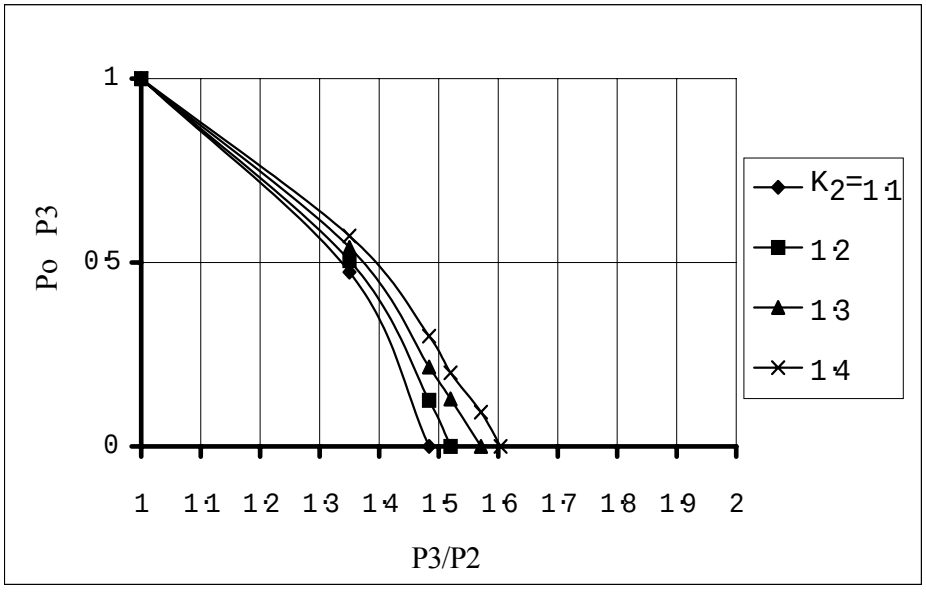

(2-3) B) to get its optimum value to be used in this to determine the optimum area, which is in agreement very well with the theoretical curves of Keenan and Neumann [4], as mentioned before.

Fig (2-3) A

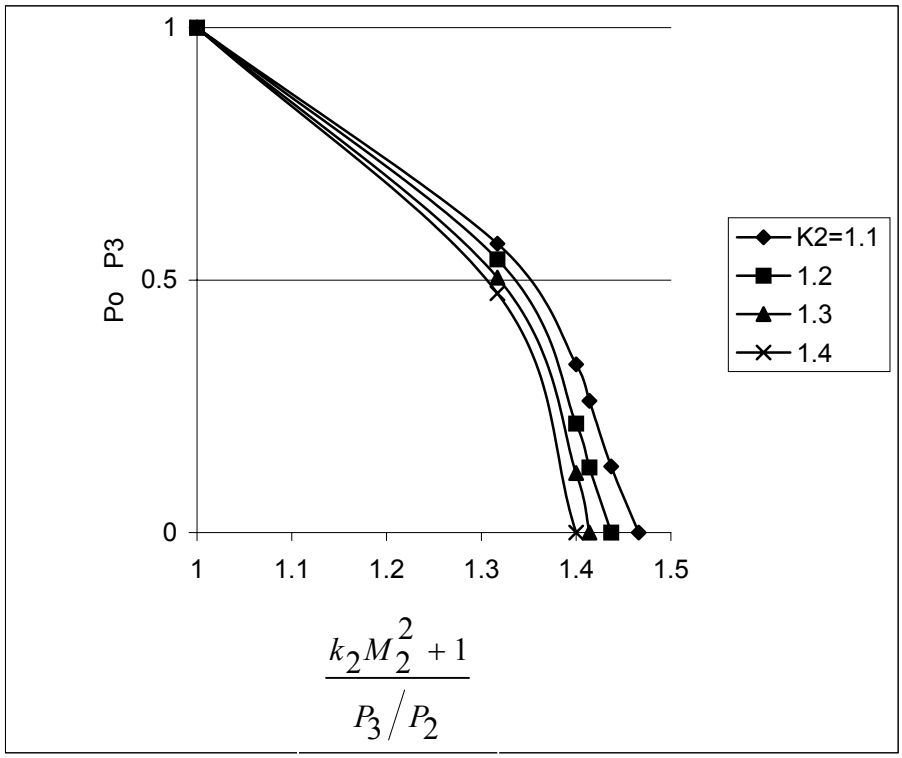

Fig (2-3) B

Keenan et al. [7] made an investigation consisting of an extension of the comparison of analytical and experimental results for a greater range of variables than that presented in reference [4]. The calculated results presented in this investigation are almost wholly confined to special cases, which are referred to as constant-pressure mixing. Air was used for the experimentation as a working fluid.

The authors found that: -

1- For the analytical conditions considered, better performance can be obtained when constant-pressure mixing is employed.
2- The total length from the nozzle exit to the entrance to the subsonic diffuser for best performance is nearly constant when the mixed stream is supersonic. The ratio of this total length to the minimum diameter is a weak function of the ratio of the nozzle inlet pressure to the suction pressure.
3- By comparison of a few experiments with the analytical results it is possible to design ejectors to accomplish a given purpose. A method for ejector design was also presented.

An attempt has been made by Engle [8] to present some of the latest developments in the design and operation of jet pumps. The design theory developed is based on the momentum exchange between motive and suction fluid and the assumption that entrainment occurs at constant-pressure and mixing at constant area.

Results showed that the nozzle was in its optimum position when it reached up to the mixing tube. For this condition the optimum mixing tube length was seven tube diameters as mentioned in ref [4] and the entry profile was found not to affect the operation.

In Gupta and Singh [9] studies, two theoretical models, one based on the momentum transport approach and the other on purely thermodynamic considerations, are presented for the design of single stage, single fluid (steam) ejector with constant pressure mixing. The results are compared with the design chart presented by Ludwig [10] as shown in fig. (2-4). The results showed that for 90.7 kg/hr of suction steam at 17.78 cm Hg.abs. Suction

pressure, the first model gave a motive steam requirement of 349 kg/hr, which compares favorably with the value of 272 kg/hr [10], whereas the corresponding figure of 156 kg/hr based on the second model is much lower.

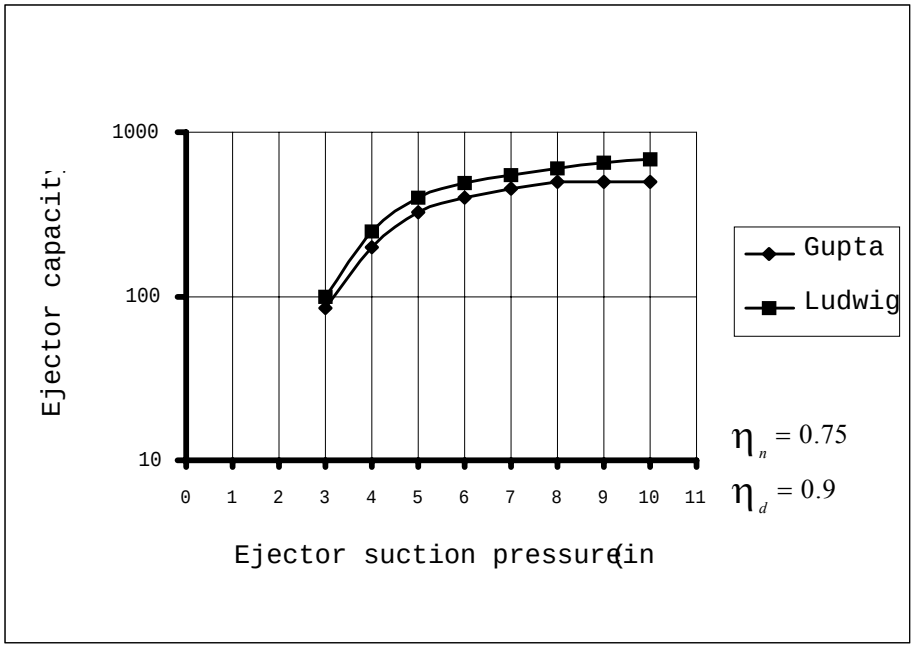

Fig (2-4) Ejector capacity with ejector suction pressure

Therefore it was concluded that the first model gives design parameters in close agreement with those obtained from available design charts which are largely empirical in nature.

To study the effect of molecular weight of on the performance of ejectors, Lincoln and Vincent [11] made an experimental study used vapors with molecular weights from 18 to 154 in two commercially manufactured ejectors, each design for a different ratio of compression and of a size suitable

for laboratory experimentation. They are each of the single nozzle and circular in cross section. It was concluded that: -

1-The variation of suction pressure with both boiler and exhaust pressure is approximately the same for all vapors, irrespective of no entrainment. The suction pressure decreases with increasing boiler pressure and fixed exhaust pressure at a variable rate down to the critical pressure ratio and then continues to decrease at a constant rate until a minimum suction pressure is attained, which is approximately the same for all vapors; beyond this point the suction pressure increases with increasing boiler pressure.

2-The weight ratio of suction vapor employed, is the same for all vapors at a given ratio of pressure, boiler to exhaust pressures, when this ratio is fixed, the efficiency of expansion, entrainment, and compression in any ejector is the same for all vapors.

3-The factors inherent in an ejector refrigeration cycle indicate that, to be highly efficient from a thermal standpoint, a system should have low molecular weights in a favorable molecular weight ratio, it should employ a boiler fluid with a low heat input requirement, with a relatively large pressure differential (exhaust pressure-suction pressure) and with a boiling point higher than that of the evaporator fluid, and it should use an evaporator fluid with a high latent heat.

A research was made by Holton, Columbus and Ohio [12], involving pumping 13 pure gases and 12 mixtures of gases with small commercial single and two-stage steam-jet ejectors supplied by two manufacturers. Results were calculated in terms of “entrainment ratio”, which is the ratio of the flow rate of gas to that of air under similar conditions. Entrainment ratios

were found to be a function of the molecular weight of the gases handled and were plotted as a smooth curve as shown in fig. (2-5), which is independent of pressure, design characteristics of ejectors, and is applicable to mixture of gases. The single smooth curve passes equally well through entrainment-ratio values obtained with both ejectors. Thus, the conclusion is reached that the curve may reasonably be used to predict results obtainable with any ejector system.

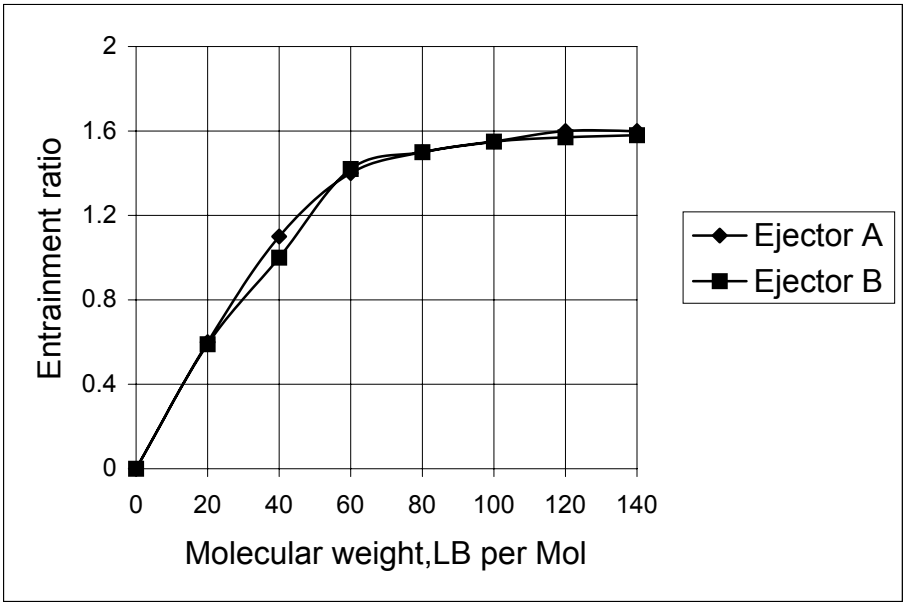

Fig. (2-5) Entrainment ratio as a function of molecular weight for pure gases and for mixtures of gases tested with two ejectors [Ref.12]

The same ejectors [12] were used by Holton and Schulz [13] to study the effect of temperature of entrained fluid on the performance of ejectors handling air and steam. The flow rate of air was calculated using the following formula recommended by HEI. [14]

$$\dot{m} = \frac{A_t C P_I}{\sqrt{R T_I}} \times 14182.9 \sqrt{\frac{k}{k-1}\left[\left(\frac{P_x}{P_I}\right)^{2/k} - \left(\frac{P_x}{P_I}\right)^{k+1/k}\right]}$$

In which

$\dot{m}$ = Mass flow rates, Ib/hr .

A_t = Area of nozzle throat, in^2 .

C = Nozzle coefficient of discharge.

P_1 = Absolute pressure at nozzle entrance, in Hg at 32 F.

P_x = Static pressure at nozzle outlet, in Hg. abs.

R = Gas constant for fluid being handled, ft. lb per (lb) (R).

T_1 = Absolute temperature at nozzle entrance, R.

k = Specific heat ratio.

The results are expressed in terms of "Entrainment ratio", which is the ratio of the flow rate of gas at a given temperature to that of the same gas at a base temperature. Entrainment-ratio was found to be a linear function of temperature as shown in fig. (2-6).

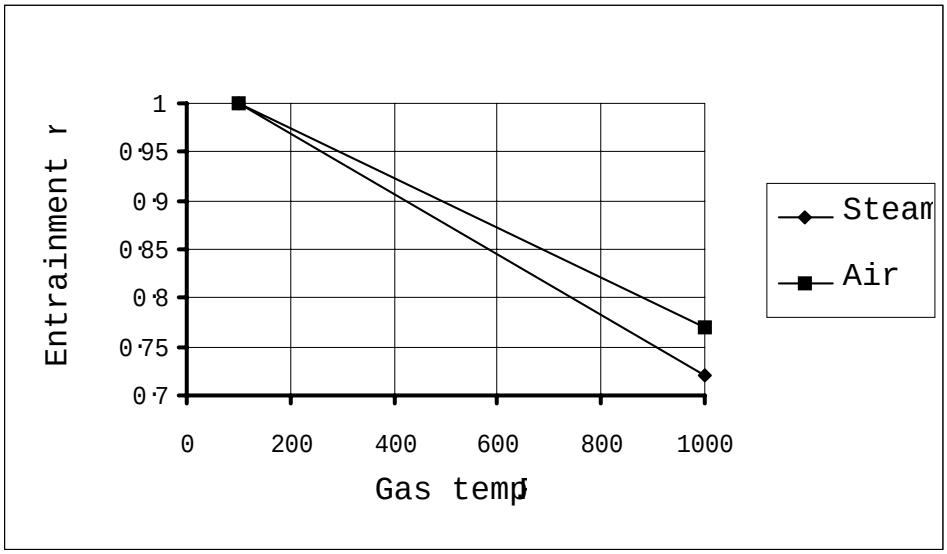

Fig. (2-6) Entrainment ratio as a linear function of temperature for air and steam with three ejectors. [Ref.13]

The test results given appear to be independent of pressure and of design characteristics of the ejectors tested. Therefore the plot of the variation of entrainment ratio with temperature is, within the limits of the accuracy, thought to be applicable to any ejector system.

Kastener and McGarry [15] studied the performance of an air ejector experimentally. The trails to determine the variation of the induced flow with the actuating flow, for the low actuating velocities (30.5 m or 61 m per second or less) and mixing angle of 2½ degree, observed that the relationship between actuating and suction velocities was very nearly a straight line as shown in fig. (2-7), and the ratio of the suction mass flow to the actuating mass flow plotted against the ratio of delivery pressure to suction pressure, for the same mixing angle. It showed that this mass ratio is approximately constant as shown in fig. (2-8).

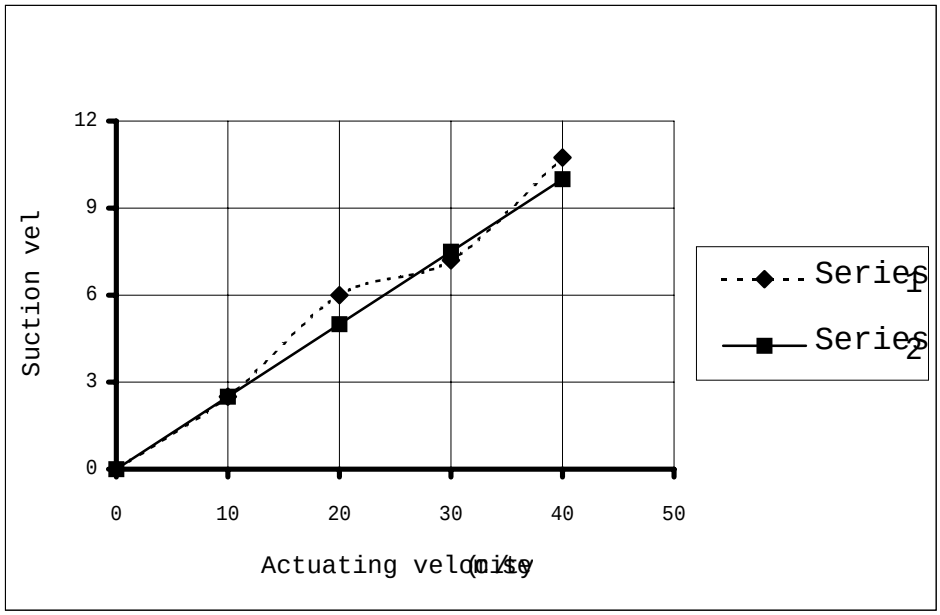

Fig. (2-7) Typical relationship between actuating and suction velocity. 2½ deg. Mixing angle [Ref.14].

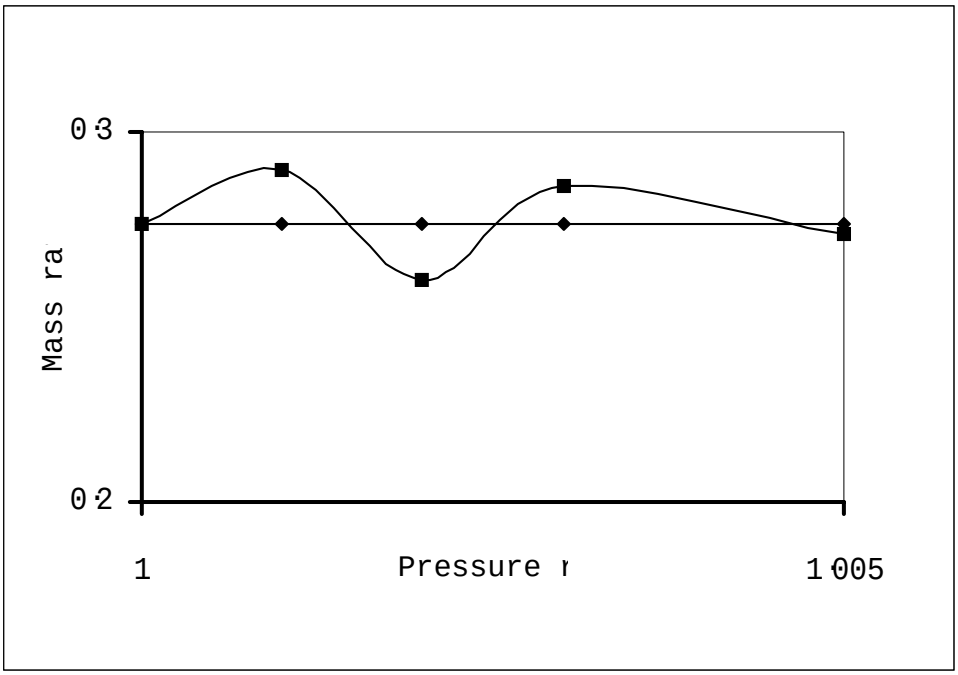

Fig. (2-8) Mass ratio versus pressure ratio. [Ref.14] 2½ deg. Mixing angle.

Dotterweich and Mooney [16] discussed the design, performance and application of the ejector in gas mixing in the natural gas industry, to entrain low-pressure gas into a stream of high-pressure gas, which must be reduced in pressure principally along delivery points in natural gas transmission line operation.

J.R. Lines of Graham Manufacturing Co. [17], Inc. attempted to show the effects on an ejector system when various operating parameters were modified in order to improve vacuum column cut point. Ejector system design was directly impacted by cut point set for the atmospheric column that precedes a vacuum column. It was noted that increasing cut point for the atmospheric column results in added stripping steam to the vacuum column, consequently, a larger ejector system is required. It was showed that by decreasing flash zone pressure within the vacuum column, whereby the column top pressure was reduced, overall utility consumption and capital cost for a revamped ejector system were favorably reduced.

For the purposes of the approach adopted herein the author have made the following process assumptions:

1. That the vacuum column diameter and mass transfer capabilities do not restrict performance.
2. That column over-head discharge diameter is not limiting column effluent capacity.
3. That modern tower internals for low-pressure drop are the basis for establishing flash zone and tower top pressure.

Fang C.Cen, Cheng-Tsang HSU [18] were studied the performance of ejector heat pumps. This paper applies the existing ejector theory to estimate the performance of an ejector heat pump system at various operating conditions. The study includes parametric, sensitivity and off- design analyses of the heat pump performance. The performance enhancement options and desired ejector geometry are also examined.

G. R. Martin, J. R. Lines and S. W. Golden [19] were studied the understand vacuum-system fundamentals. They were the Crude vacuum unit heavy vacuum gas-oil (HVGO) yield was significantly impacted by ejector-system performance, especially at conditions below 20 mmHg absolute pressure. A deep cut vacuum unit, to reliably met the yields, calls for proper design of all the major pieces of equipment. Understanding vacuum ejector system impacts, plus minimizing their negative effects equals maximum gas yield. Ejector-system performance could be adversely affected by poor upstream process operations.

The impacts of optimum ejector performance were more pronounced at low flash-zone pressures. Gas-oil yield improvements for small incremental pressure reductions were higher at 8 mmHg than at 16 mmHg. Commercial operation of a column with a 4.0 mmHg top pressure and 10 mmHg flash-zone pressure is possible.

Ejector Have a Wide Range of Uses was presented by F. Duncan Berkeley [20] Ejector were simple pieces of equipment. Nevertheless many of their possible services were overlooked. They often were used to pump gases and vapors from a system to great a vacuum.

Ejectors were employed in the industry in numerous, unique and even sometimes bizarre ways. They used singly or in stages to create a wide range of vacuum conditions, or they operated as transfer and mixing pumps. The ejectors had the following advantages over other kinds of pumps: Rugged and simple construction, Capability of handling enormous volumes of gases in relatively small sizes of equipment, Less maintenance requirements and Simple operation.

W. D. Mains and R. E. Richenberg [21] were studied the steam jet ejector in pilot and production plants. Steam jet ejector are employed in the chemical process industries and refineries in numerous and very often unusual ways. They provide, in most cases, the best way to produce a vacuum in these process plants because they were rugged and of simple construction therefore, easily maintained. Their capacities varied from the very smallest to enormous quantities. Because of their simplicity and the manner of their construction, difficulties were unusual under the most extreme conditions. They were simple to operate. Ejectors which were properly designed for a given situation were very forgiving of errors in estimated quantities to be handled and of upsets in operation and were found to be easily changed to give the exact results required. In pilot plant operations all of these were important functions, because in a pilot plant a great deal of information was usually unknown, and something must be selected which will operate over a very wide range.

Therefore, this article will outline the differences between ejectors for a pilot plant and those for a production plant, pointing out that pilot plant ejectors were not just small editions of production plant ejectors.

***Objective**: -*

The objective of the present work is to carry out a theoretical analysis for a steam-jet refrigeration system operating at a range of evaporating temperature, condensing temperature, boiler temperature, and at different throat areas and develop computer program to obtain the results shall be illustrated in chart form to allow designers to select parameters at optimum or near optimum performance

Optimum performance of a system is defined when the largest (C.O.P.) at a given operating conditional (pressure and temperature of generator, evaporator and condenser).

Chapter three

Theoretical Analysis

3.1 Introduction

An ejector heat pump cycle in its simple form, as illustrated in figure (3-1), is a combined cycle, which consists of a power cycle and a refrigeration cycle. It differs from the conventional Rankine refrigeration cycle in which the mechanical compressor is replaced by an ejector. The power cycle of an ejector heat pump includes a boiler, an ejector, a condenser and a liquid pump. In addition to an expansion valve and an evaporator, the refrigeration cycle shares the ejector and the condenser with the power cycle. Flow compression work, produced in the power cycle by absorbing heat at the boiler and by rejecting residual heat to an intermediate temperature at the condenser, is transferred to the refrigeration cycle at the ejector. This drives the compression process to allow the low temperature heat to be absorbed at

the evaporator, upgraded to an intermediate temperature, and discharged through the condenser.

Since the ejector heat pump is thermally activated, low-grade thermal resources such as solar-heated water or industrial waste heat can be used as the heat source. Alternatively, it can be driven by a gas-fired furnace.[17]

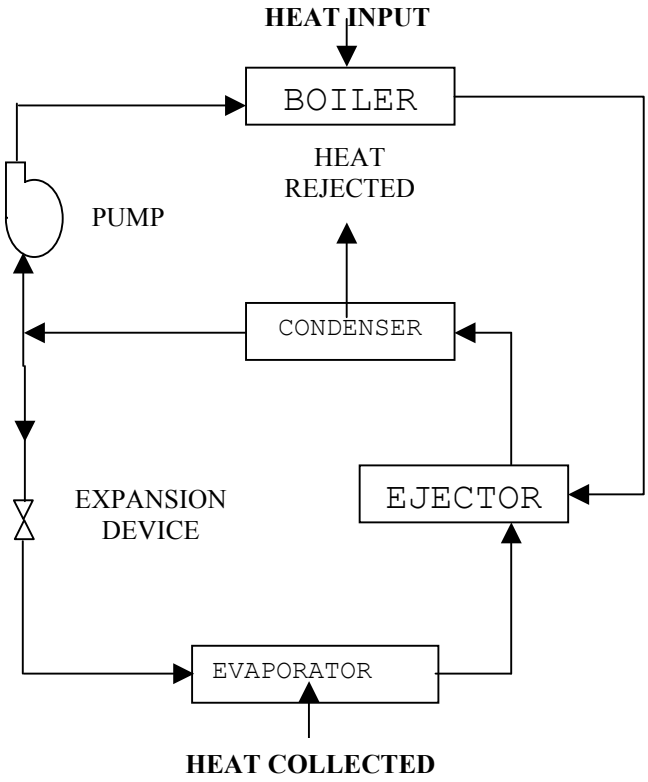

Figure.3-1 An ejector heat pump cycle.

3.2 Description of the model

3.2.1 Evaporator: -

The evaporator is usually a large volume vessel which must provide a large water surface area for efficient evaporative cooling action. Water sprays figure (3-2) and cascading water in sheets figure (3-3) are two common means of maximizing water surface. The design of an evaporator requires the water to be distributed in small droplets or thin sheets so that the main body of the water can attain equilibrium temperature by the time it reaches the bottom of the evaporator. The vapor space in the evaporator must provide a volume for the vapor to freely separate from the liquid at a velocity sufficiently low to prevent liquid carry over into the booster suction. Spray systems are more susceptible to water carry over problems than cascade-type systems. It is important to keep pressure losses to a minimum between the point of vapor release from the water and the steam ejector suction. Since ejectors are inherently inefficient compression devices, the compression work must be minimized for maximum efficiency.

Evaporators can be further divided into two types: -

1. The open chilled water system, in which the refrigerant water from the evaporator is circulated directly to the cooling load, such as heat exchanger or other equipment, which must be cooled.
2. The closed chilled water system, in which the refrigerant water is recirculated within the evaporator over a coil or other heat transfer device through which is circulated another fluid (water or brine is commonly used) which never mixes with the refrigerant water and which in turn is pumped to the cooling load.

The open chilled water system is more efficient because one less stage of heat transfer is required. For the same chilled water temperature, the refrigerant water temperature :(i.e.; evaporator) can be 3 to 5.5 C^0 (5 to 10F) higher using the open system.[18]

Evaporator freezeup may occur in steam-jet system when certain controls malfunction. The open system has two distinct advantages in such situation. First, the 3 to 5.5 C^0 higher refrigerant water temperature means that the system has a greater safety margin above the possible freeze level. Second, should freezeupn actually occur, there is no danger of tube rupture, which is certain to occur in the closed system. Some applications with special process requirements, however, necessitate the use of a closed water system to isolate the chilled water system.[18]

The open system must be carefully designed to avoid leaks. It is recommended that the chilled water in open systems be pumped sufficiently above atmospheric pressure so that the water returning to the evaporator will be at 7 to 12 kPa. This will both prevent air from leaking into the pressure side of the system and prevent vapor lock in the piping. The returning water is introduced into the evaporator through a backpressure valve in such a case. [18]

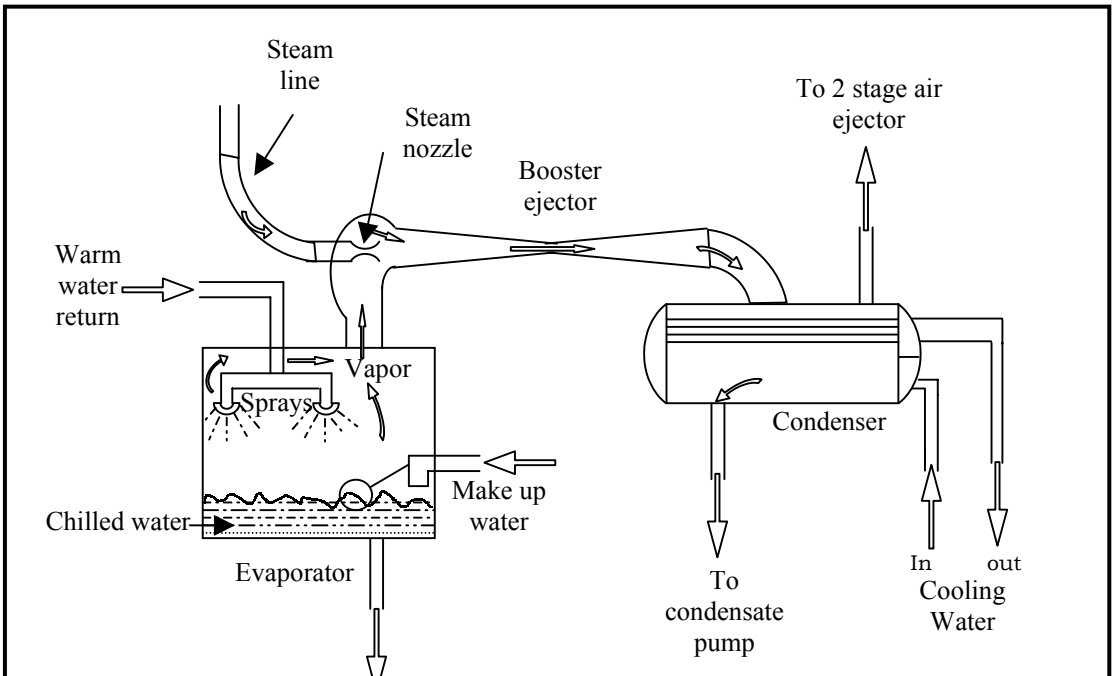

Figure 3-2 Steam-jet refrigeration system with surface condense

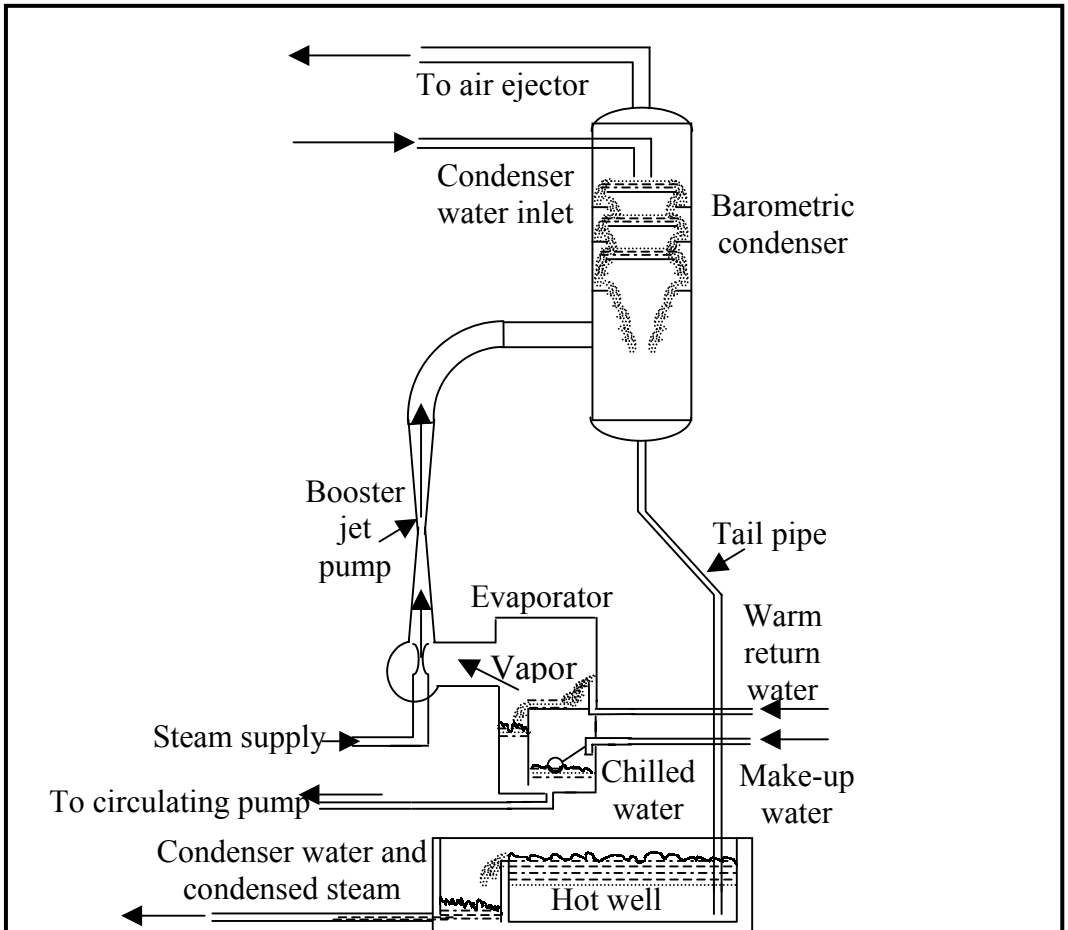

Figure 3-3 Steam-jet refrigeration systems with Barometric Condenser

3.2.2 Condenser: -

The condenser can be one of three basic types: (1) conventional surface condenser, (2) an evaporative condenser, or (3) barometric condenser.

The conventional surface condenser is commonly selected because of its compact size and ability to be located anywhere, including inside a building figure (3-3). When a natural supply of cooling water is not available (i.e.; river, well, ocean, etc.), a cooling tower must be employed. Use of a cooling tower will rise the condensing temperature above that which would be necessary if either an evaporative or barometric condenser were used, so the steam consumption will be correspondingly higher and a larger surface condenser and cooling water system will be necessary.

The evaporative condenser contains tubes in which the steam from ejector condenses. Forced air is drawn over the tube bundle, upon which water is sprayed or otherwise distributed to produce the condensing effect through vaporization of water from the outer tube surface. Such condensers were used in railway car steam-jet refrigeration units of 18 to 25 kw (5 to 7 Tons) capacity during the late 1930s and are now available in more modern, larger capacity units. However, since such condenser cannot be located indoors, they are limited to outdoor installations. The evaporative condenser operates with or at condensing temperature 2 to $4\,C^0$ below that of a surface

condenser with cooling tower; this in turn results in favorable decrease consumption. [18]

The barometric (or contact) condenser is used to advantage in installation, which do not have space limitations (primarily vertical), and where it is economically feasible to treat the evaporator and boiler water on a once-through basis figure (3-4).

The unit provides low first cost. Since cooling water mixes directly with the steam to condense it, a closer approach between cooling water temperature and condensing temperature results than would be found in either a surface or evaporative condenser. [18]

3.2.3 Boiler:

The steam boiler capacity depends on the maximum mass flow rate that received by the ejector. And the types of the boilers that can be used are *Fire tube boiler* and *Water tube boiler.*

3.2.4 Steam-jet ejector:

The steam-jet ejector is the heart of the steam-jet refrigeration cycle. The characteristics of this component have a major effect on the operating cost of the system and the size of both the condenser and the condenser cooling water system.

A steam ejector is shown in figure (3-4). The Terminology of the heat exchange institute is given, but, in addition, the sections are identified functionally. [18]

The high-pressure steam used to energize the ejector is called the primary fluid or motive steam. The induced steam, which is to be raised to a higher-pressure level, is the secondary fluid; it is often referred to as vapor. The motive steam is expanded through a converging-diverging nozzle to velocities of the order of 1200 m / s. the corresponding nozzle pressure ratio

is very high. For example, a nozzle expanding 1030 kpa absolute pressure motive steam to an evaporator pressure of 1 kpa absolute (7.2 C^0 chilled water temperature) will have a pressure ratio of about 1000. Nozzle pressure ratios less than 200 are uncommon due to poor ejector efficiency when operating at low steam pressures.

The high velocity steam issuing from the nozzle entrains the water vapor leaving the suction chamber, and the two streams merge in the mixing section, which is usually conical in shape, converging in the direction of flow.

Theoretically, mixing is assumed to occur at constant pressure and, therefore, at constant total momentum per unit time. For a typical steam-jet ejector in a refrigeration cycle, the mean velocity of the mixture will be supersonic (after mixing is complete). The most efficient way to recover the kinetic energy in a supersonic vapor stream is to decelerate it to just above sonic velocity then let it undergo a compression shock to just below supersonic velocity followed by a subsonic deceleration to exit velocity. The typical ejector design attempts to achieve this recovery by providing a constant area throat section following the mixing section. This, in turn, is followed by a diverging section, (such a design is illustrated in figure (3-4). [18]

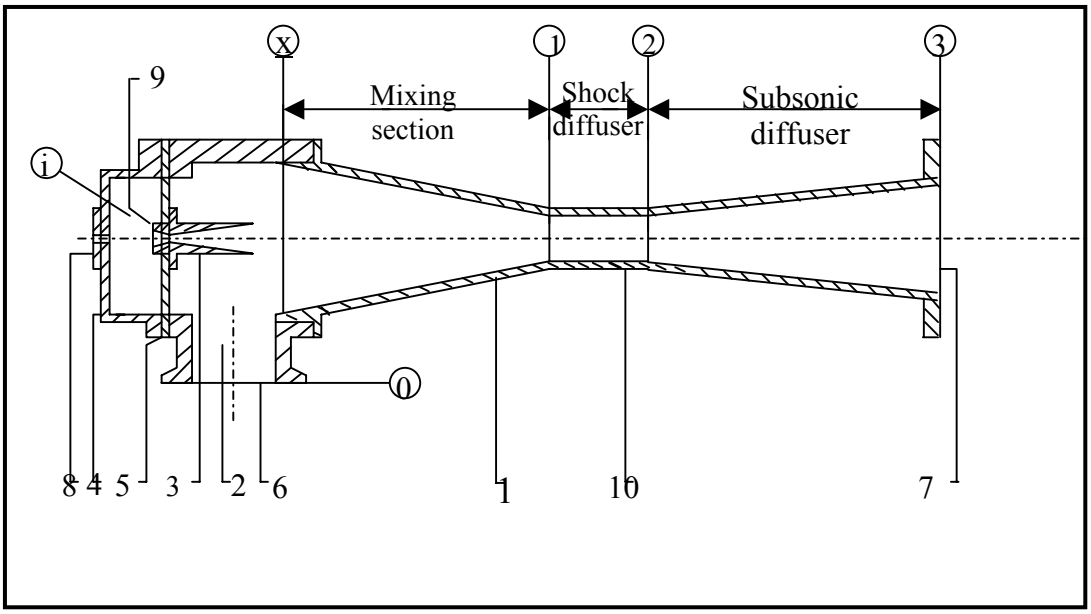

1. Diffuser.
2. Suction chamber.
3. Steam nozzle.
4. Steam chest.
5. Nozzle plate.
6. Suction.
7. Discharge.
8. Steam inlet.
9. Nozzle throat.
10. Diffuser throat.

Figure.3-4 Basic Steam-Jet Ejector or Booster Assembly.

3.3 General Assumptions: -

For the theoretical analysis of steam-jet refrigeration system, the following general assumptions are applied:

- Both motive steam as well as the secondary vapor enters the ejector at essentially saturated condition.

- Flow separation inside the ejector nozzle or in the secondary inlet does not occur.
- Heat transfer and friction losses to the wall and mixing losses are neglected (isentropic flow).
- The process of mixing in the mixing section is constant pressure mixing process. Also the static pressure of the exit of the nozzle is the same of that of the suction section.
- To eliminate analytical errors induced by the assumption of an ideal gas for ejector, the thermodynamics properties are directly introduced from steam table.
- The system without precooler and pregenerator.

3.4 Design considerations: -

Not much material on the physical Design of efficient steam ejectors has been published. Although many papers pertaining to ejector design have been written, most have been concerned with analysis of air–to–air, steam–to air, or other combinations, and their applicability to steam– jet refrigeration systems is questionable. The majority of papers in the literature describe the best ejector of a particular investigative series; unfortunately, these have rarely, if ever, been as efficient as commercially available ejectors [18]. It is therefore undesicable to utilize or rely on the design data generally found in the literature as a basis for an efficient ejector design. Nevertheless, much valuable work is recorded in the literature, which contributes a better understanding of ejector design problems. The reluctance of ejector manufacturers to publish design data is understandable, since they have evolved their design through decades of costly experimentation. This relative secrecy implies that ejector design is more of an art than a science, which is,

in fact, the situation at the moment. A major contribution to the science of ejector Design has been the paper by Keenan, Neumann, and Lustwerk [18]. While this is a one-dimensional ideal analysis, it is very useful in describing a logical mathematical model of ejector operation. The most extensive discussion is that by Johannesen. [18]

3.4.1 Nozzle

The motive steam Nozzle has a characteristic convergent divergent shape. Its throat is sized to give the desired steam flow at the design inlet steam conditions. The nozzle's divergent section is typically conical in shape and the theoretical area ratio (cone outlet area to the throat area) is found through conventional supersonic flow equations [18]. The cone angles (total included angle) employed in the divergent nozzle cone range from 8 to 15 degree, with 10 to 12 degree most common.

The theoretical area ratio and an assumed design divergent cone angle will define the theoretical length. However, experience has shown that in practice the cone length at the design cone angle should be reduced to 70 to 80% of the theoretical length for a broader efficiency characteristic of the ejector. This arises from the need of the ejector to operate at off-design conditions. It has been found [18] that it is more efficient to operate the ejector when the last portion of the expansion process in the divergent nozzle section takes place at or beyond the exit plane of the cone than when the expansion process is completed within the cone itself, giving rise to a normal shock at this point. Such a condition would arise both at an evaporator temperature higher than design and at startup if no shortening of the cone took place.

The nozzle axis must coincide with the main ejector axis. The nozzle is usually mounted so that its axial position relative to the inlet of the mixing

section at Station x of figure (3-4) can be varied to achieve optimum performance. It can be shown in tests that the use of superheated motive steam causes a slight decrease in ejector efficiency.

While saturated steam is the most efficient motive steam condition for ejector operation, such a steam condition is difficult to control because of heat losses. Since drops of wet steam can cause serious erosion of both nozzle and main ejector parts due to the very high velocities encountered, a few degrees of superheat are often used to effectively eliminate the erosion hazard from ejector. In actual installations, erosion is virtually nonexistent. Good thermal insulation on the steam lines and good steam trapping practices also help eliminate erosion.

3.4.2 Ejector suction opening and suction chamber: -

The ejector suction opening is generally sized to give an average vapor velocity of about 76m/s (250 fps) .the suction chamber is a volume in which the entering water vapor is turned 90 degree and accelerated to some optimum velocity at station x figure (3-4). It can be shown both theoretically [18] and experimentally that there is an optimum velocity of the vapor entering the mixing section at station x for every ejector design condition. Typically, the vapor velocity increase as the design pressure ratio of the ejector (condenser to evaporator pressure) decreases. For steam-jet refrigeration units tied to comfort air-conditioning systems, the vapor velocity is typically 120 to 180 m/s (400 to 600 fps) at station x (based on evaporator state conditions).

3.4.3 Mixing section

The Mixing section is conical in shape. For refrigeration application, most ejector manufacturers normally use a double cone in series arrangement, with the larger included angle cone starting at station x and the smaller cone

ending at station 1. The length of the Mixing section is often expressed in terms of throat diameters at station 1 to station 2. For steam jet refrigeration work, the Mixing section will be 6 to 10 throat diameters long, with an average value of 7. It can be shown theoretically [18] and by test that the optimum mixing section cone angle decreases with decreasing ejector design pressure ratio. For a design pressure ratio of one, the cone angle becomes zero and a cylindrical constant area mixing section results. For the typical steam–jet ejector on refrigeration service, the included angles of the mixing section cone are about 7 to 10 degree for the first portion and 3 to 4 degree for the second portion. Larger angles will result in the ejector being unable to compress design vapor flow to the design condensing pressure.

3.4.4Constant area section: -

The Constant area section is the supersonic shock diffuser section (stations 1-2). In an ideal one–dimensional analysis, the pressure rise in this section might be expected to take place across a normal shock of essentially zero axial length. This is not the real situation. Because of a thick boundary layer and a very peaked velocity profile (as opposed to the ideal case of no boundary layer and a uniform velocity profile), the shock is not fully normal but includes complex oblique shock patterns [18] as well, and in practice several throat diameters of axial length are required to complete this portion of the pressure recovery process [18].

During load variation, this complex and lengthy shock patterns shifts axially. For a broad and efficient ejector operating characteristic, this constant area throat section is typically three to five throat diameters long to accommodate the shock patterns and its axial movement under load. The constant area section diameter is critical for a specific design and, although the literature gives several methods for computing this dimension, none is

precisely accurate [18]. Only ejector manufacturers possess data with which to accurately predict the throat diameter for ejectors of all sizes and operating requirements.

3.4.5 Subsonic diffuser: -

The Subsonic diffuser is always conical in shape with an included angle range of 5 to 12 degree, although 8 to degree are most common. An axial length of four to 12 throat diameters is found in practice, with a five-diameter length most common. A small included angle of 5 to 7 degree would be more efficient if sufficient axial length were available to decelerate the flow to the typical average leaving velocity of 76 m/s (250 fps) at station 3 figure (3-4). However, ejector manufacturers have attempted to standardize ejector sizes and usually employ cone angles greater than 7 degree to keep within length limitations, which are often quite arbitrary.

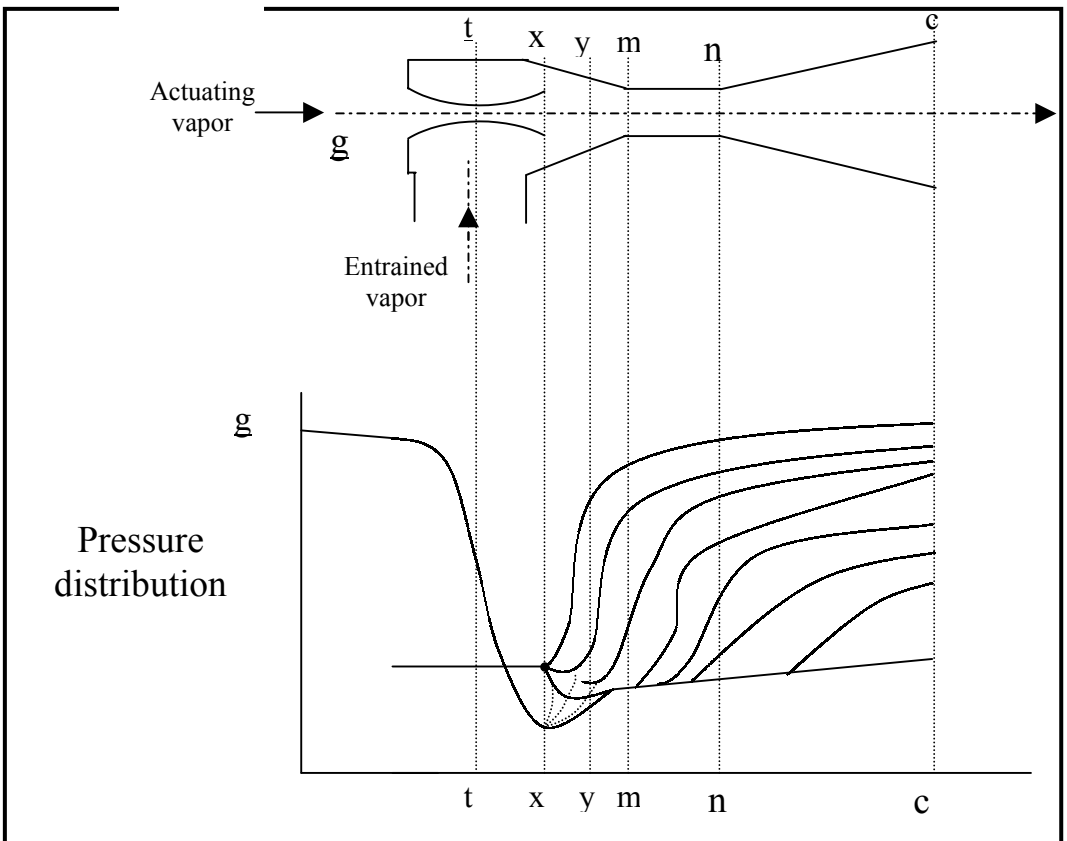

Figure 3-5 pressure variations inside the ejector.

3.5 Controls: -

The control of a steam-jet unit are usually relatively simple compared to other types of refrigeration systems. The evaporator water level and the condenser hot-well level are usually controlled by liquid level control devices, such as float valves. A thermostatic control of the chilled water temperatures can be applied to operate the steam-jet unit (or, in multiple ejector applications, sequential activation) in an on-off mode. [18]

3.6 Analysis of system components: -

Based on the above assumptions, the following analysis is applied.

3.6.1Ejector efficiency: -

A Mollier diagram and the schematic diagram of an ejector with its corresponding state points for an ejector heat pump are shown in Figure (3-6). The high-pressure motive gas is the refrigerant vapor supplied from the boiler. At state point 0 the total pressure corresponds to the boiler pressure, p_b . From there, the motive gas expands through the nozzle to a static pressure,

p_e (evaporator pressure), at state point 1, which is located to the right of the isentropic expansion location 1_s. The low-pressure refrigerant vapor (secondary gas) from the evaporator enters the ejector at a total pressure p_e corresponding to state point 4. The two streams are merged at x and completely mixed at state point 2. The combined refrigerant vapor is self-compressed through the diffuser section and then leaves the ejector at state point 3, which is located to the right of state point $3'$ of the isentropic compression. The total pressure of state point 3 corresponds to the condenser pressure, p_c.

The ratio of the secondary mass flow rate to the primary mass flow rate may be defined as the entrainment rate. For given inlet conditions and outlet presser of the working fluids, there is a maximum ideal value of entrainment rate attainable by an ejector. This ideal entrainment rate can be used as a criterion of ejector performance. Therefore, the efficiency of an ejector can be defined by [17]

$$\eta_E = \frac{acual \quad entrainment \quad rate}{ideal \quad entrainment \quad rate} \tag{3-1}$$

The ideal entrainment rate may be derived by assuming the reversible processes of expansion, mixing and compression of the refrigerant vapor throughout the ejector. If the inlet and outlet conditions of the refrigerant are prescribed and the overall changes of kinetic and potential energy are negligible, the conservation of energy requires that

$$\dot{m}_o h_o + \dot{m}_4 h_4 = (\dot{m}_o + \dot{m}_4) h_3 \tag{3-2}$$

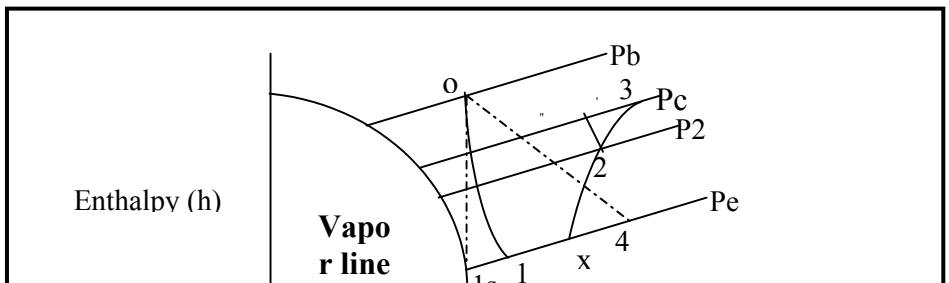

Figure 3-6 Mollier diagram for an ejector heat pump system

The isentropic process requires that

$$\dot{m}_o s_o + \dot{m}_4 s_4 = (\dot{m}_o + \dot{m}_o)_{s_3} \qquad \textbf{(3-3)}$$

If both primary and secondary gases are of the same species, it has been shown (Chen, 1978) that the ideal entrainment rate can be determined graphically on the Mollier diagram (Figure 3-6). The state point $3''$ is the ideal exit condition, which satisfies equations (3-2, 3). The ideal entrainment rate, $(\dot{m}4/\dot{m}0)$s, can be expressed as the ratio of the length of the line $\overline{03''}$ to the length of line $\overline{3''4}$.

However, it is cumbersome to construct a Mollier diagram and measure the relevant lengths. Instead, the ideal entrainment rate is calculated using a trial-and-error solution with an existing refrigerant property computer program (Kartsounes and erth, 1971; Hsu, 1984).

3.6.2 Optimum ejector analysis: -

The actual entrainment rate of an ejector depends on many factors, including the ejector operating conditions optimum mixing section area, A_2, can be found by maximizing $\dot{m}_4$ subject to the governing equations which are shown below

Mass flow rate through the nozzle-throat area is obtained from continuity equation [21]:

$$\dot{m} = \rho \times V \times A \tag{3-4}$$

Mach number is

$$\because M = \frac{V}{a} \tag{3-5}$$

Where $$a = \sqrt{kRT} \tag{3-6}$$

Substitute equation (3-6) in (3-5)

$$\therefore V = M \times \sqrt{kRT} \tag{3-7}$$

And from equation of state [21]:

$$\rho = \frac{P}{RT} \tag{3-8}$$

Substitute equations (3-7) and (3-8) in (3-4)

$$\therefore \dot{m} = \frac{P}{RT} \times \sqrt{kRT} \times A \tag{3-9}$$

By using Energy equation [21]:

$$\frac{dE}{dt} = \frac{\partial}{\partial t} \iiint_{c.v.} e \times \rho \times d\forall + \iint_{s} e(\rho \times V \times dA) \tag{3-10}$$

$$= \frac{dQ}{dt} - \frac{dW}{dt}$$

If the system total energy is divided between internal, kinetic, and potential energy, as defined by [21]

$$E = U + K.E. + P.E.$$

Then

$$e = u + \frac{1}{2}V^2 + gz \tag{3-11}$$

$u =$ Internal energy per unit mass

Now, Substitute equation (3-11) in (3-10)

$$\frac{\partial}{\partial t}\iiint_{c.v.} e \times \rho \times d\forall + \iint_{s}\left(u + \frac{1}{2}V^2 + gz\right)(\rho \times V \times dA) = \frac{d}{dt}(Q - W) \tag{3-12}$$

From thermodynamic properties [21]:

$$h = u + \frac{P}{\rho} \tag{3-13}$$

Substitute equation (3-13) in (3-12)

$$\frac{\partial}{\partial t}\iiint_{c.v.} e \times \rho \times d\forall + \iint_{s}\left(h + \frac{1}{2}V^2 + gz\right)(\rho \times V \times dA) = \frac{d}{dt}(Q - W) \tag{3-14}$$

The energy equation with no external heat transfer and no work, becomes, for steady one-dimensional flow.[21]

$$\iint_{s}\left(h + \frac{1}{2}V^2\right)(\rho \times V \times dA) = 0 \tag{3-15}$$

$$dh + d\frac{V^2}{2} = 0 \tag{3-16}$$

At the control volume

$$h_t = h + \frac{1}{2}V^2 \tag{3-17}$$

But,

$$h_t - h = Cp(T_t - T) \tag{3-18}$$

$$\therefore T_t = \frac{V^2}{2 \times Cp} + T = T\left(1 + \frac{V^2}{2 \times Cp \times T}\right) \tag{3-19}$$

$$\because Cp = \frac{k \times R}{k - 1} \tag{3-20}$$

From equations (3-19) and (3-20) find:

$$T_t = T\left[1 + \frac{(k-1) \times V^2}{2kRT}\right] \tag{3-21}$$

$$\because a^2 = kRT \tag{3-22}$$

And from equation (3-5) were,

$$M^2 = \frac{V^2}{a^2} \tag{3-23}$$

Now, Substitute equation (3-22) and (3-23) in (3-21)

$$T_t = T\left[1 + \frac{(k+1)}{2} \times M^2\right] \tag{3-24}$$

For a perfect gas with constant specific heats undergoing an isentropic process[21]:

$$\frac{P_2}{P_1} = \left(\frac{T_2}{T_1}\right)^{k/(k-1)} \tag{3-25}$$

For stagnation state:

$$\frac{P_t}{P} = \left(\frac{T_t}{T}\right)^{k/k-1} \tag{3-26}$$

By using equation (3-24) we find that:

$$\therefore \frac{P_t}{P} = \left(1 + \frac{k-1}{2} \times M^2\right)^{k/(k-1)} \tag{3-27}$$

By using equation (3-24) and (3-27) we find that the mass flow rate is:

$$\dot{m} = \frac{P_t}{\sqrt{RT_t}} A\sqrt{k} M \left(1 + \frac{k-1}{2} M^2\right)^{(k+1)/(2-2k)} \tag{3-28}$$

For maximum mass flow rate through the throat area when chocked flow at Mach number =1. [21]

$$\therefore \dot{m}_o = P_t \left[\frac{k}{RT_t}\right]^{1/2} \times \left[\frac{k+1}{2}\right]^{(k+1)/(2-2k)} \times A_{th} \tag{3-29}$$

where $P_t = P_b$ & $T_t = T_b$.

From figure (3-6) Nozzle efficiency is[17]

$$\eta_n = \frac{h_o - h_1}{h_o - h_{1s}} \tag{3-30}$$

By using equation (3-17) and substitute equation (3-30) we find that the velocity of the primary fluid at the nozzle exit is

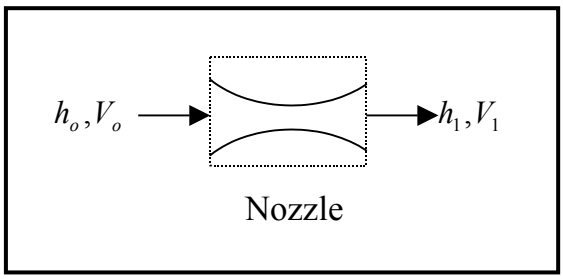

Figure (3-7) The Control volume of the nozzle

$V_o = 0$, Stagnation flow in the boiler.[17]

$$\therefore V_1 = \left[2\eta_n \left[h_o - h_{1s}\right]\right]^{0.5} \tag{3-31}$$

Flow through the mixing section

From the control volume as shown in figure (3-8):

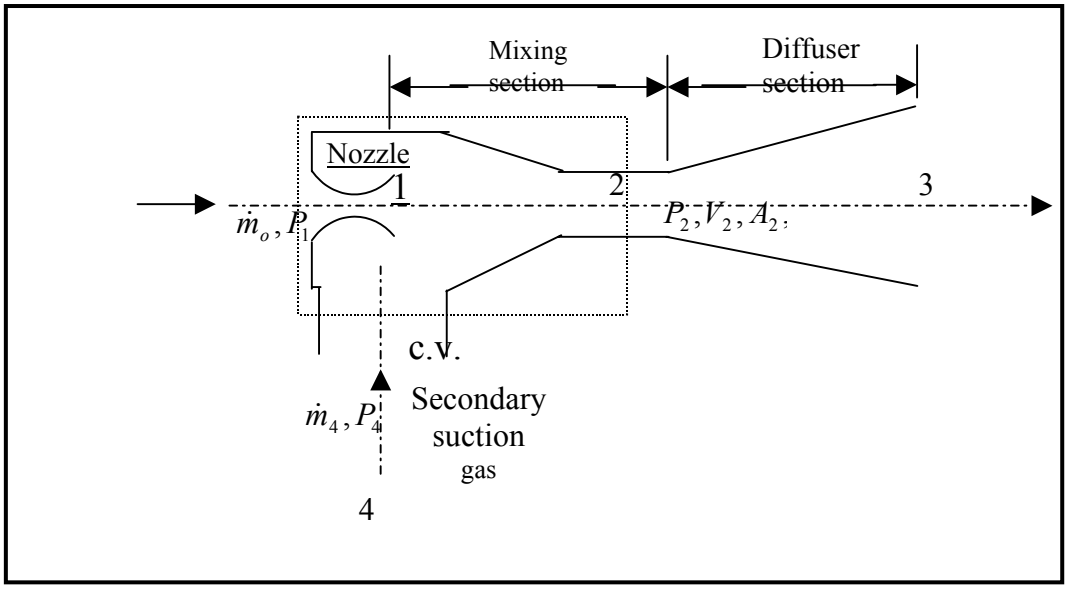

Figure (3-8) the control volume of input and output from the mixing section.

The continuity equation:

$$\sum_{in} \dot{m} = \sum_{out} \dot{m} \tag{3-32}$$

Becomes.

$$\dot{m}_o + \dot{m}_4 = A_2 V_2 / v_2 \tag{3-33}$$

The Momentum equation for this control volume becomes.[ ]

$$\dot{m}_o V_1 + P_4 A_2 = (\dot{m}_o + \dot{m}_4) V_2 + P_2 A_2 \qquad (3\text{-}34)$$

And the Energy.[17]

$$\dot{m}_o h_o + \dot{m}_4 h_4 = (\dot{m}_o + \dot{m}_4)(h_2 + V_2^2/2) \qquad (3\text{-}35)$$

Where $P_4 = P_e = P_1$.

The criterion for an optimized ejector, derived by Elrod (1945), is as follows[17]:

$$M_2^2 \left[1 + (1 - \eta_d) \frac{T_2}{T_{3'}} \left[\left[\frac{d\left[\ln \frac{T_2}{v_2} \right]}{d(\ln v_2)} \right]_s + \frac{k}{1 - P_4/P_2} \right] \right] = 1 \qquad \textbf{(3-36)}$$

Applying ideal gas and isentropic process relations, equation (3-36) may be simplified to.[17]

$$M_2^2 \left[1 + (1 - \eta_d) \left(\frac{P_2}{P_3} \right)^{\frac{k-1}{k}} \left[\frac{k}{1 - P_4/P_2} - k \right] \right] = 1 \qquad \textbf{(3-37)}$$

Where $P_3 = P_3'$, and the energy equation in the diffuser section (equation (3-35)) can be expressed as.[17]

$$\left(\frac{P_3}{P_2}\right)^{\frac{k-1}{k}} - \eta_d M_2^2 (k-1)/2 = 1 \qquad \textbf{(3-38)}$$

For given values of η_d, k, P_3 and P_4, equations (3-37) and (3-38) can be solved simultaneously to obtain M_2 and P_2 (within the range of interest of $0<M_2<1$). Thus, the optimum mixing section area, A_2, with respect to a unit nozzle-throat area can be obtained by substituting these values into equation (3-42).

Flow through the diffuser

From the control volume for the diffuser as shown in figure (3-9) find:

Energy.[17]

$$h_2 + V_2^2/2 = h_3 \qquad (3\text{-}39)$$

Diffuser efficiency equation.[17]

$$h_{3'} - h_2 = \eta_d (h_3 - h_2) \qquad (3\text{-}40)$$

Where state $3'$ has coordinates P_3 and S_2.

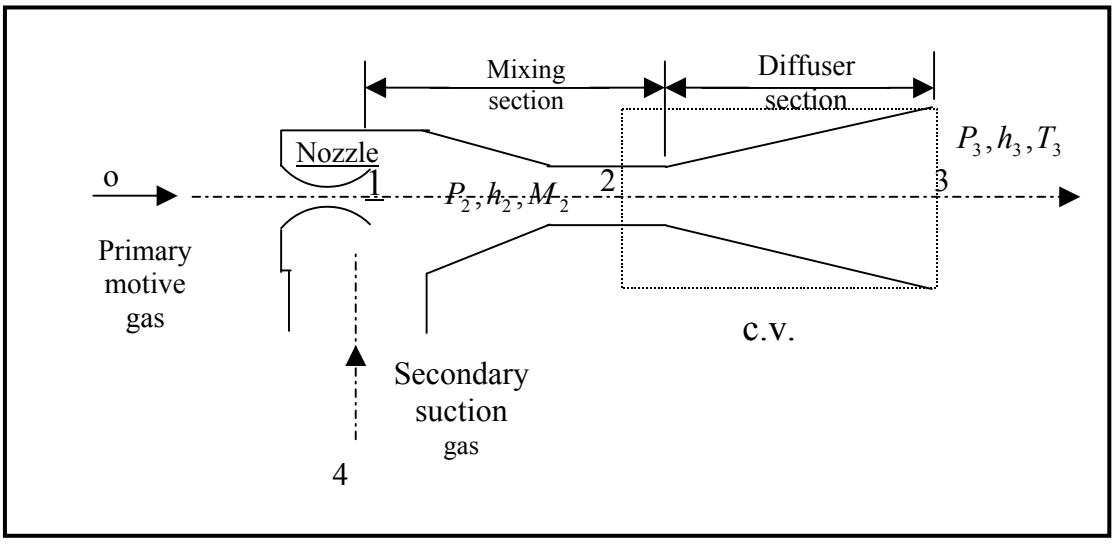

Figure (3-8) the control volume of the diffuser.

The mixing section area

Let M_2 = Mach number at section 2, and for a perfect gas

$$M_2 = V_2 / (kP_2 v_2)^{0.5} \tag{3-41}$$

From equations (3-33), (3-34) and (3-41), the cross-sectional area, A_2, may be solved by.[17]

$$A_2 = \frac{\dot{m}_o V_1}{P_2 (kM_2^2 + 1) - P_4} \tag{3-42}$$

For the unit area of nozzle throat.

3.6.3 Ideal cycle performance[17]: -

From thermodynamics, a Carnot cycle machine will give the maximum thermal efficiency for an engine and the maximum COP for a refrigerator. It has been shown (Hamner, 1978;Chen, 1978) that a reversible ejector heat pump cycle is a combination of a Carnot engine cycle operating between the boiler and the condenser temperatures, and a Carnot refrigeration cycle operating between the condenser and the evaporator temperatures. The ideal system COP for cooling can then be derived as [17]

$$\text{Ideal } COP_C = \frac{(T_b - T_c)}{T_b} \frac{T_e}{(T_c - T_e)} \tag{3-43}$$

Similarly, the ideal COP for an ejector heat pump heating cycle can be derived as 1 plus the ideal cooling COP. it is equal to the efficiency of a

Carnot engine operating between the temperatures T_b and T_e multiplied by the COP for a Carnot heat pump operating between the temperatures T_c and T_e.

3.6.4 Non-ideal cycle calculations[17]: -

In reality, an ejector heat pump will be operating in a less-than ideal environment with thermodynamic irreversibility's including imperfect energy transfer and flow friction losses.

Anon-ideal ejector heat pump in cooling mode is assumed to operate at a boiler temperature of nearly to 100^0C, a condenser temperature of about 45^0C, and an evaporator temperature of 10^0C. The T-S diagram of ejector heat pump cycle is shown in Figure 3.The boiler, condenser and evaporator are assumed to operate at saturation pressures corresponding to the given temperatures. With the assumed values of specific heat ratio k=1.4(taken at 30^0C and 1 atmosphere), diffuser efficiency η_d=0.5 and nozzle efficiency η_n=0.97,the non-ideal ejector heat pump cycle performance with an optimized ejector for the given operating condition can be calculated from equations (3-1)-(3-38).

The results and the procedure for a sample calculation are summarized in Table (3-1).

The pump work of the liquid refrigerant is small, about 1 per cent of the equivalent thermal energy input. The COPs of the non-ideal cycle are calculated according to the definition of coefficient of performance: [17]

$$(COP)_c = \frac{cooling\quad energy\quad sought}{energy\quad that\quad costs} = \frac{\dot{m}_4(h_4 - h_7)}{\dot{m}_o(h_o - h_5)} = 0.638 \qquad (3\text{-}44)$$

$$(COP)_h = \frac{heating\quad energy\quad sought}{energy\quad that\quad costs} = \frac{(\dot{m}_4 + \dot{m}_o)(h_3 - h_5)}{\dot{m}_o(h_o - h_5)} = 1.638 \qquad (3\text{-}45)$$

These values are sought to be more representative of the actual performance of an ejector heat pump. The ratios of actual COPs to their ideal value are 26 per cent for the cooling cycle and 60 percent for the heating cycle.

Table (3-1) A sample cycle calculation of the steam jet refrigeration system

At Boiler temperature =100^{o}C,

Condenser temperature =50^{o}C,and

Evaporator temperature =5^{o}C

Calculation results	Determined by
$M_2 = 0.9689$	Equations (3-37) and (3-38)
$P_2 = 0.0091 Mpa$	Equations (3-37) and (3-38)
$h_{1s} = 2045.19 kJ/kg$	S_o and P_4
$V_1 = 1223.7 m/s$	Equation(3-31)
$R = 416 J/kgK$	
$A_{th} = 0.005 m^2$	Assumed
$\dot{m}_o = 0.8215 kg/s$	Equation (3-29)
$A_2 = 0.0513 m^2$	Equation (3-42)
$S_2 = 8 J/kgK$	Initial assumed value
$h_2 = 2523.05 kJ/kg$	S_2 and P_2
$v_2 = 15.67 m^3/kg$	S_2 and P_2
$h_{3'} = 2567.45 kJ/kg$	S_2 and P_3
$h_3 = 2611.85 kJ/kg$	Equation (3-40)
$V_2 = 421.42 m/s$	Equation (3-39)
$\dot{m}_4 = 0.52 kg/s$	Equation (3-2)
$(\dot{m}_o + \dot{m}_4)/A_2 = 26.15 kg/sm^2$	Satisfy Equation (3-33), otherwise another S_2 must be assumed to repeat the calculations.
$V_2/v_2 = 26.89 kg/sm^2$	
$\dot{m}_4/\dot{m}_o = 0.633$	
$P_3/P_4 = 14.1954$	
$(\dot{m}_4/\dot{m}_o)_s = 1.484$	
$(COP)_{c-ideal} = 0.638$	
$(COP)_{h-ideal} = 1.638$	
$\eta_E = 0.4265$	Equation (3-1)

To compare with the steam jet refrigeration system we made the calculations to an equivalent system like an Absorption system works at the same conditions of elements temperature and capacity as shown in table (3-2)

Table (3-2) A sample of calculation to the Absorption system

At generator temperature =100^{o}C,

Condenser temperature =50°C,

Evaporator temperature =5°C, and

Absorber temperature=30°C.

Calculation results	Determined by
$q_e = 2301.5 \times w_3$	From equation (C-4)
$q_e = 1374kW$	given
$w_3 = 0.597kg/s$	
$w_1 - w_2 = 0.597$	From equation (C-1)
$x_1 = 0.54$	From figure (C-2) at $T_{ev} = 5^o C$
$x_2 = 0.62$	From figure (C-2) at $T_{con} = 50^o C$
$w_1 = 1.148 \times w_2$	From equation (C-2)
$w_1 = 4.033kg/s$	
$w_2 = 4.63kg/s$	
$q_g = 2229.3kW$	From equation (C-3)
$COP_c = 0.616$	From equation (C-5)

Chapter four

Results and Discussion

Analysis and results obtained are based on the assumptions considered in section of this work

4.1 <u>The variation of the system characteristics with boiler temperature at various throat areas.</u>

4.1.1 Effect of boiler temperature on primary vapor flow rate.

Fig (4-1) shows the variation of primary vapor flow rate when boiler temperature is varied at different throat areas, taking into consideration that evaporating and condensing temperatures are 5 and 45C^{o} respectively. The vapor flow rate ($\dot{m}_o$) indicated in the figure represents the maximum flow through a chocked nozzle at the various operating conditions. For the condition indicated above, the mass flow rate is obtained using equation (3-28) in which it may be observed that ($\dot{m}_o$) varies directly with boiler pressure and throat area and inversely with the temperature. This may be attributed to the fact that the increase in boiler pressure for a given condensing back pressure results in higher flow through the nozzle due to varying pressure distribution while the throat remains chocked and the ratio of boiler to throat pressure remines constant.

Also for a given boiler temperature and pressure, larger throat area requires higher flow rate in order to reach chocking conditions.

Attempts are made to represent, mathematically, the relation between primary flow rate and boiler temperature required to chock a given throat area. The curve fitting lines and equations for the conditions of figure (4-1) are illustrated in figure (4-2). This figure shows excellent agreement between results and curve fitting lines.

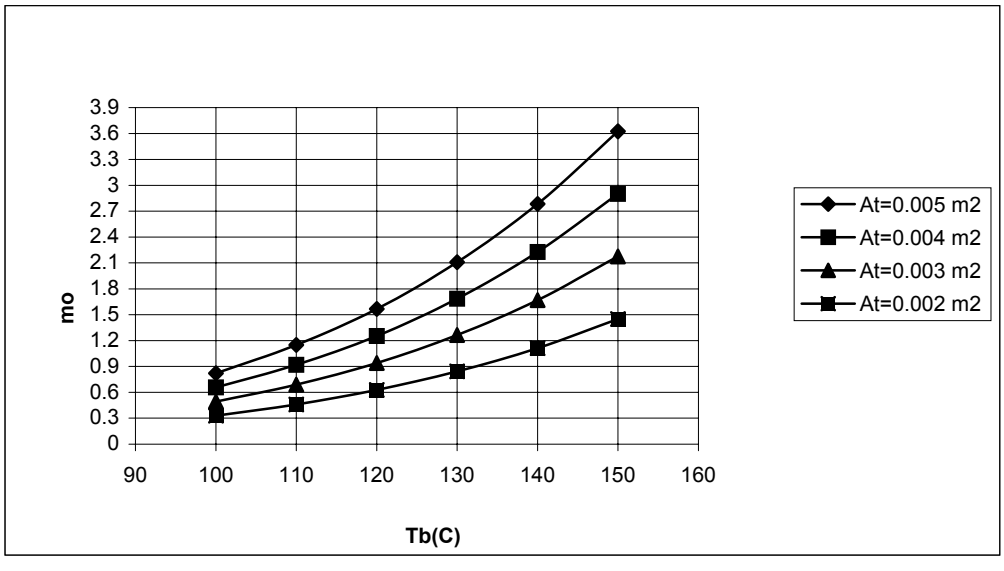

Fig (4-1) variation of boiler mass flow rate with boiler temperature at different throat areas ($T_{con} = 45^o C, T_{ev} = 5^o C$)

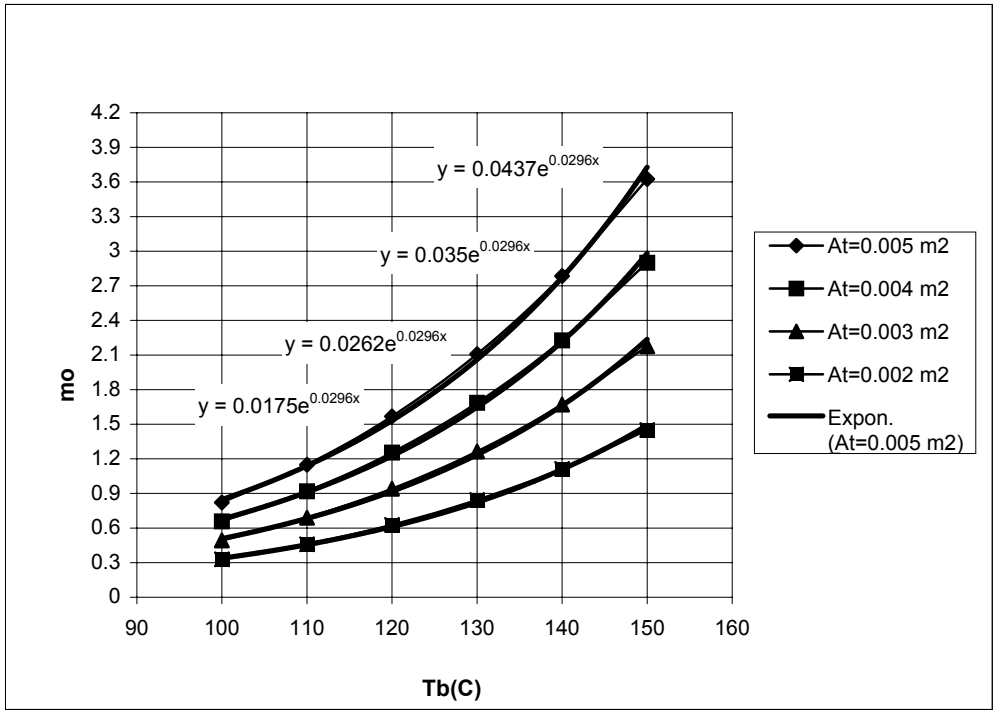

Fig (4-2) Curve fitting equations representing primary vapor flow rate at different boiler temperature and throat areas ($T_{con} = 45^o C, T_{ev} = 5^o C$)

4.1.2 Effect of the boiler temperature on secondary vapor flow rate.

Fig (4-3) shows the variation of secondary vapor mass flow rate ($\dot{m}_4$) emanating from the evaporator with boiler temperature (T_b) at different throat area (A_t) and for the evaporating and for the evaporating and condensing condition indicated in the figure. It can be seen that the secondary vapor mass flow rate ($\dot{m}_4$) increases with boiler temperature (T_b) increase and throat area increase. As seen in figure (4-1) that primary vapor flow rate is in direct proportion to boiler temperature and pressure. From conservation of mass, the increase in mass flow rate through a fixed geometry nozzle results in higher

flow velocity. The momentum equation shows that the velocity gradient is indirectly proportion to pressure gradient, i.e. when the velocity increases the pressure decreases, hence exit pressure. The result obtained and shown in figure (4-3) and curve fitted as shown in figure (4-4) and the resulting equations are indicated.

$$\dot{m}_4 = 5\times10^{-11}\times T_b^{\,5.0252}$$

$$\dot{m}_4 = 4\times10^{-11}\times T_b^{\,5.025}$$

$$\dot{m}_4 = 1\times10^{-9}\times T_b^{\,4.2301}$$

$$\dot{m}_4 = 9\times10^{-10}\times T_b^{\,4.2326}$$

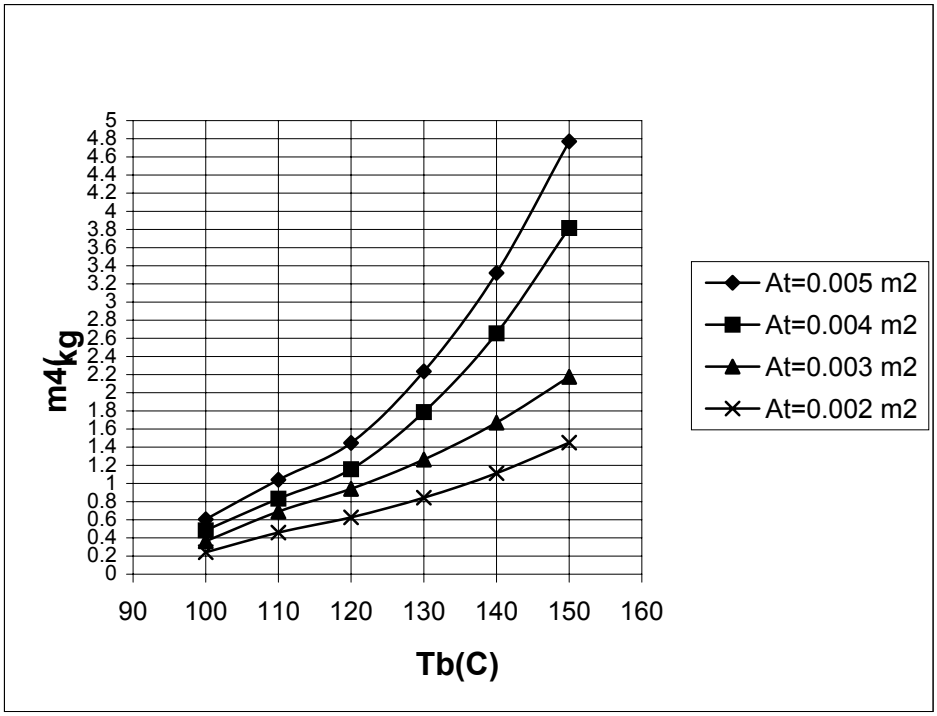

Fig (4-3) variation of evaporate mass flow rate with boiler temperature at different throat areas($T_{con} = 45^{o}C, T_{ev} = 5^{o}C$)

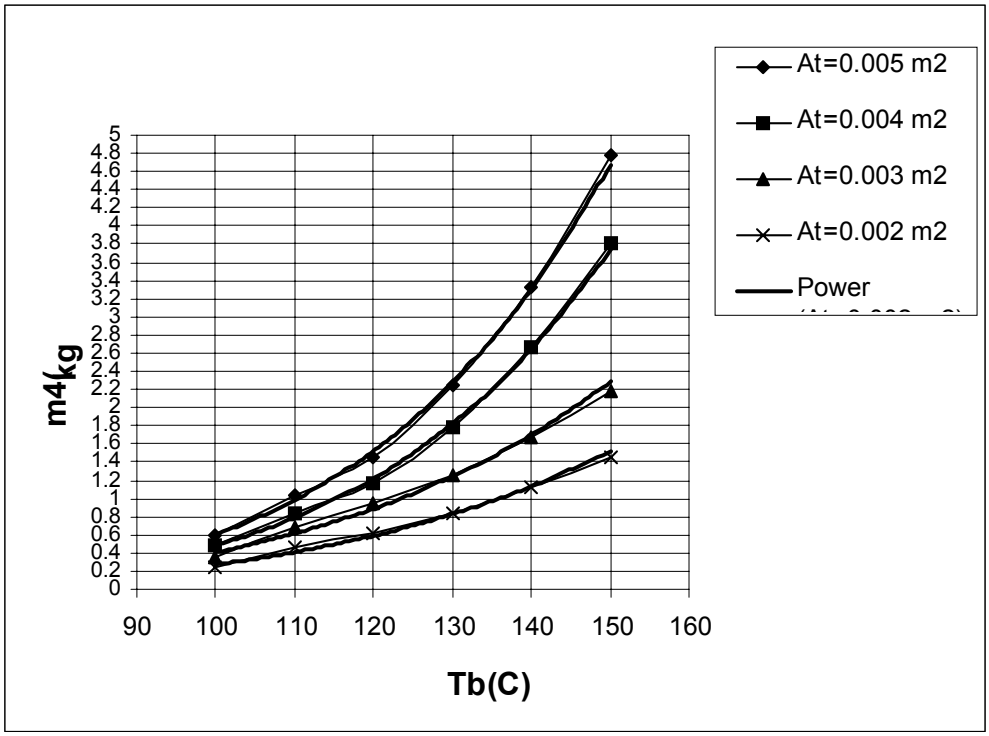

Fig (4-4) The curve fitting for the variation of evaporate mass flow rate with boiler temperature at different throat areas ($T_{con} = 45^{o}C, T_{ev} = 5^{o}C$)

4.1.3 Effect of the boiler temperature on the cooling Coefficient of performance.

Fig (4-5) shows variation of cooling coefficient of performance (COP_c) of the system with boiler temperature at the conditions illustrated in the figure and different throat areas. It can be seen that the cooling coefficient of performance of the system increase with the increase of boiler temperature. This can be attributed to the fact that the entrainment ratio ($\dot{m}_4/\dot{m}_o$) increases as the boiling temperature increases, refer to equation number (3-8). At the same time the enthalpy ratio appearing in the equation was found to decrease with increased boiling temperature, but the entrainment ratio effect is dominant. The relation between the cooling coefficient of performance and saturated boiling temperature is curve fitted and the fallowing equation was deduced:

$$COP_c = -3\times10^{-6}\times T_b^{\,3} + 0.0014\times T_b^{\,2} - 0.1692\times T_b + 7.3807$$

It is of interest to see that the (COP_c) is not that area dependent hence it is the same whatever is the capacity.

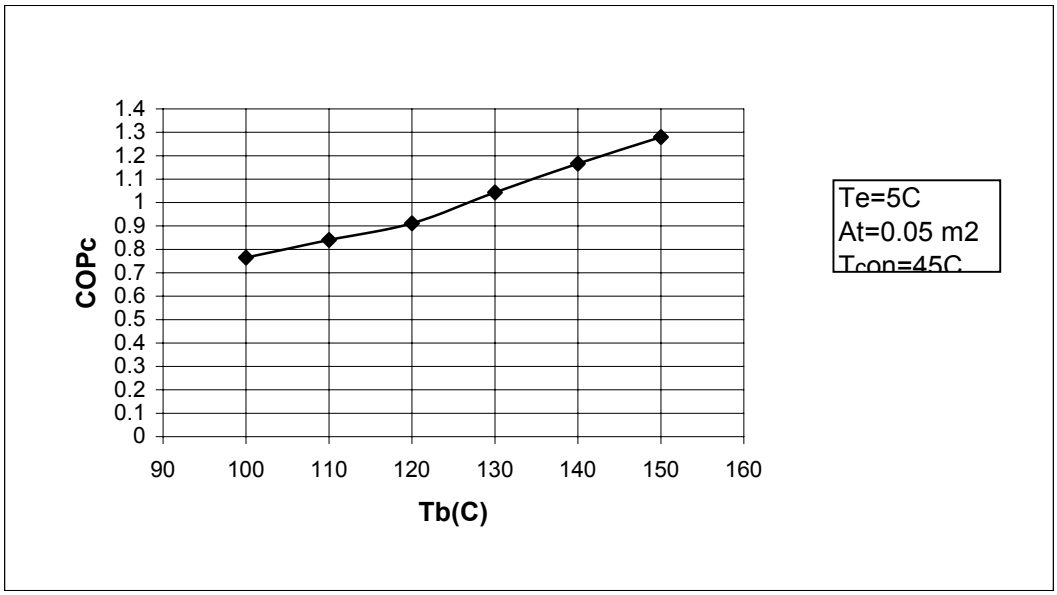

Fig (4-5) variation of cooling Coefficient of performance with boiler temperature at different throat areas ($T_{con} = 45^{o}C, T_{ev} = 5^{o}C$)

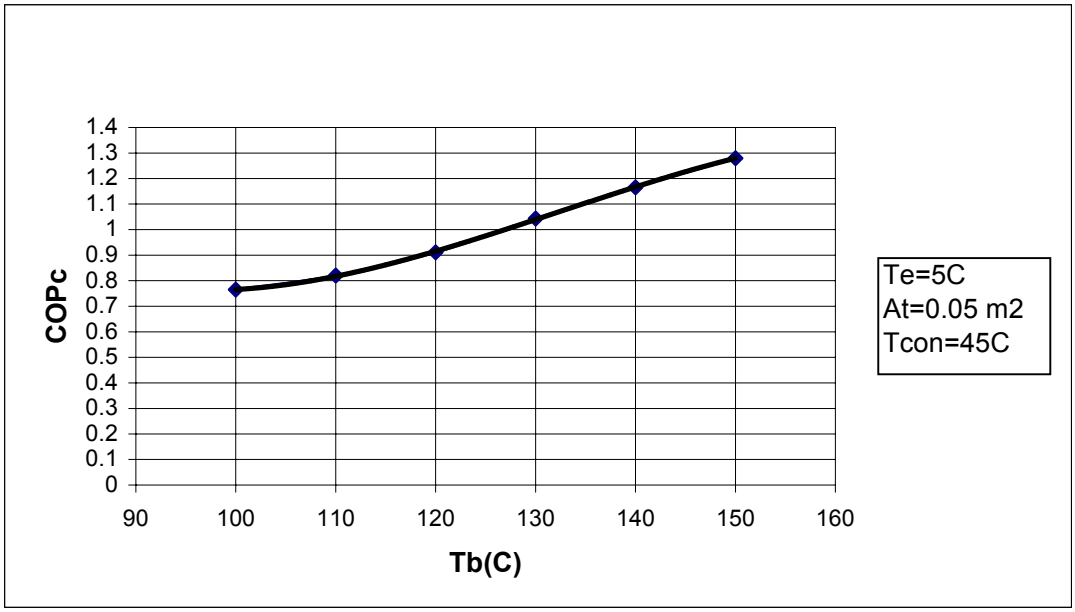

Fig (4-6) The curve fitting for the variation of cooling Coefficient of performance with boiler temperature at different throat areas ($T_{con} = 45^{o}C, T_{ev} = 5^{o}C$)

4.1.4 Effect of the boiler temperature on the system capacity.

Fig (4-7) shows variation of system capacity (Q) with boiler temperature (T_b) at different throat areas with evaporating and condensing temperatures as indicated. It can be seen that the capacity increases with boiler temperature rise and throat area enlargement. Both boiler temperature rise and larger throat area result in higher evaporator vapor flow rates, which means higher system capacity. The result obtained and shown in figure (4-7) and curve fitted as shown in figure (4-8) and the resulting equations are indicated.

$$Q = 1\times10^{-7} \times T_b^{\,5.0256}$$

$$Q = 1\times10^{-7} \times T_b^{\,5.0251}$$

$$Q = 4\times10^{-6} \times T_b^{\,4.229}$$

$$Q = 2\times10^{-6} \times T_b^{\,4.2321}$$

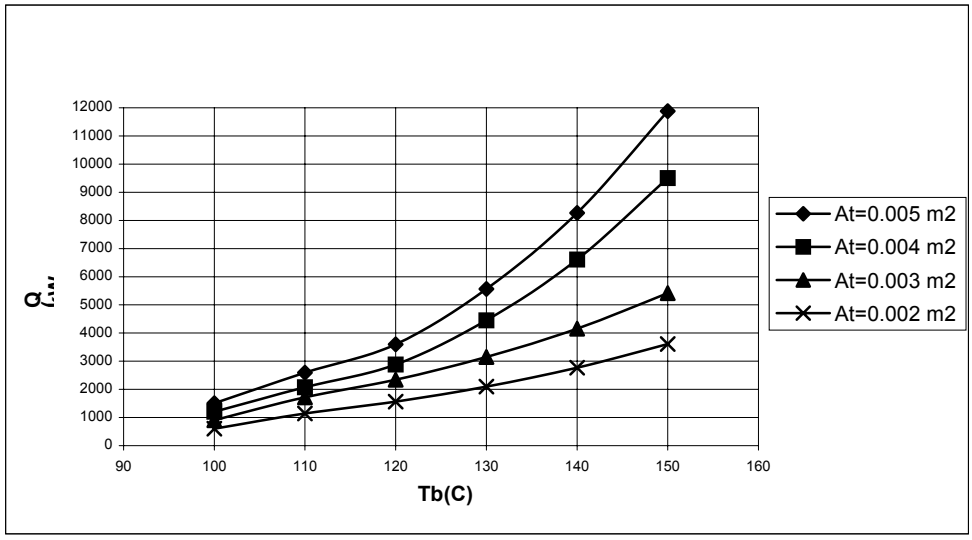

Fig (4-7) variation of system capacity with boiler temperature at different throat areas ($T_{con} = 45^o C, T_{ev} = 5^o C$)

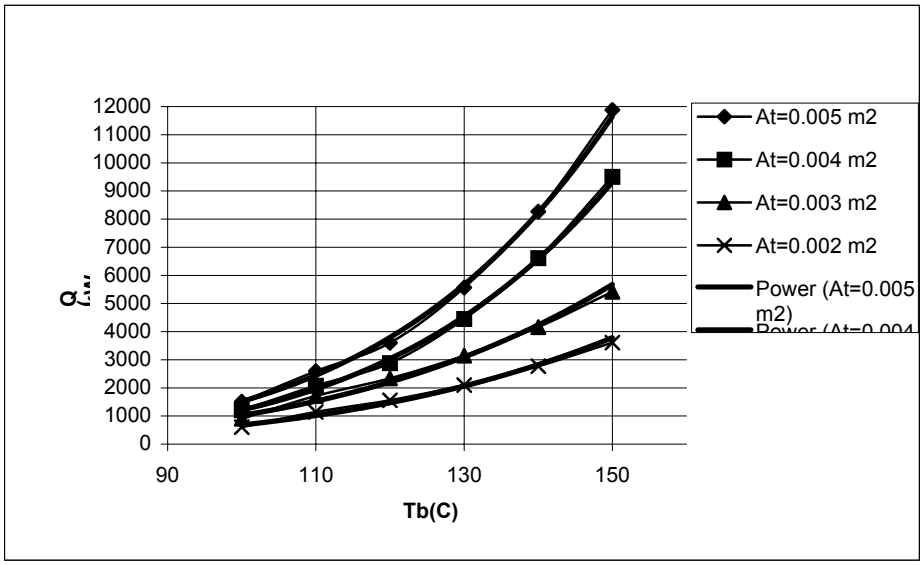

Fig (4-8) The curve fitting for the variation of system capacity with boiler temperature at different throat areas ($T_{con} = 45^{o}C, T_{ev} = 5^{o}C$)

4.1.5Effect of the boiler temperature on the heating Coefficient of performance.

Fig (4-9) shows variation of heating coefficient of performance of the system with boiler temperature at conditions illustrated in the figure at different throat areas. It can be seen that the heating coefficient of performance of the system increases with the boiler temperature rise. And it may be seen that the (COP_h) at any boiling temperature is higher than (COP_c). And this may be explained by examining equation (3-44). Both equation are identical except that equation (3-45) includes ($\dot{m}_o$) in the numerator in addition and that results in a difference of unity between the two $C.O.P.s$. The result obtained and shown in figure (4-9) and curve fitted as shown in figure (4-10) and the resulting equations are indicated.

$$COP_h = 0.0835 \times T_b^{0.6481}$$

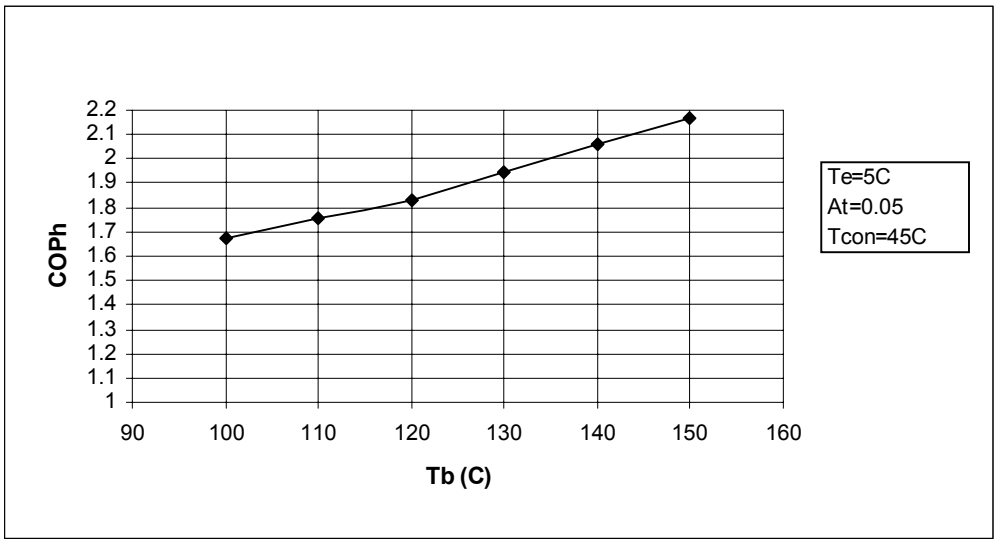

Fig (4-9) variation of heating Coefficient of performance with boiler temperature at different throat areas ($T_{con} = 45^o C, T_{ev} = 5^o C$)

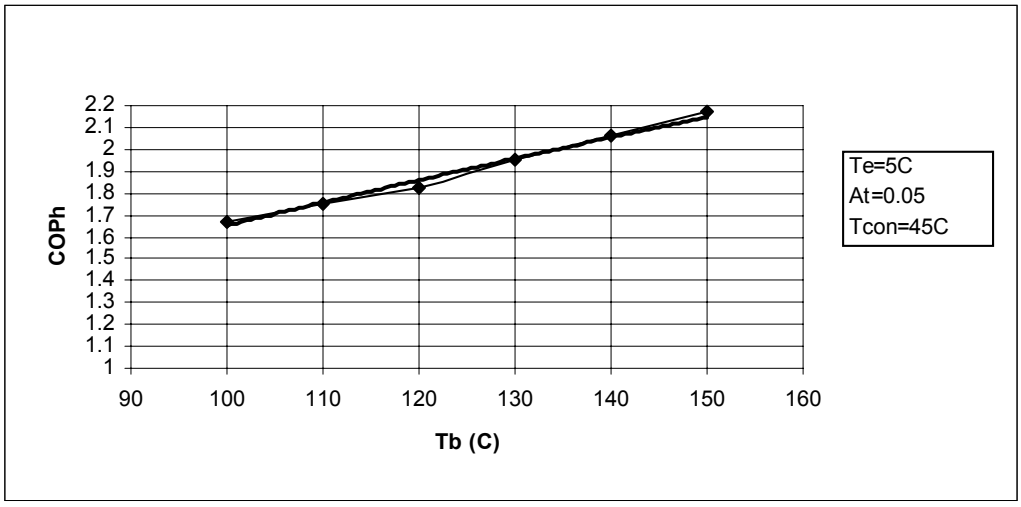

Fig (4-10) The curve fitting for the variation of heating Coefficient of performance with boiler temperature at different throat areas ($T_{con} = 45^o C, T_{ev} = 5^o C$)

4.2 The variation of the system characteristics with condenser temperature at different throat areas.

4.2.1 Effect of the condenser temperature on the evaporator mass flow rate.

Fig (4-11) shows variation of evaporator flow rate with condenser temperature at different throat areas at conditions illustrated in the figure. The figure shows that appreciable drop in entrained vapor flow rate when the condenser pressure is allowed to rise. This is due to the effect of back pressure rise in back pressure while boiler pressure is maintained results in lower boiler vapor flow rate. Since the entrained vapor flow rate. Since the entrained vapor flow rate varies directly with motive vapor, it will eventually decrease, as motive vapor is less.

Figure (4-11) also shows that for a given condensing temperature the entrained vapor flow rate is higher at bigger throat area. This is also due to the higher boiler motive vapor flow rate with bigger throat areas.

The results obtained are curve fitted and illustrated in figure (4-12) and obtained on the below equations.

$$\dot{m}_4 = 5.6403 \times T_{con}^{-0.5895}$$

$$\dot{m}_4 = 4.5956 \times T_{con}^{-0.5942}$$

$$\dot{m}_4 = 3.3811 \times T_{con}^{-0.5893}$$

$$\dot{m}_4 = 2.2714 \times T_{con}^{-0.5913}$$

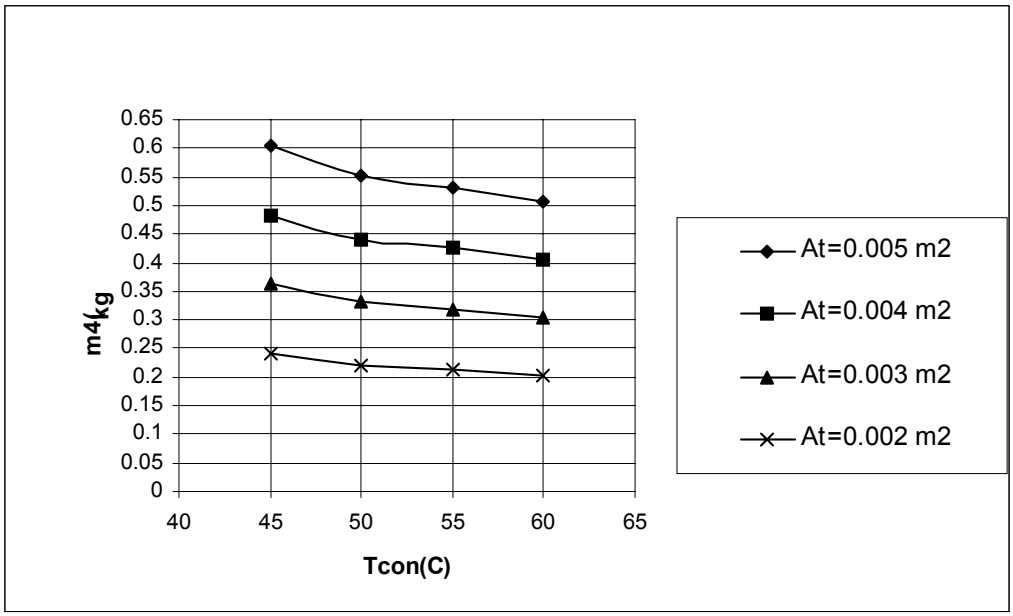

Fig (4-11) variation of evaporate mass flow rate with condenser temperature at different throat areas ($T_b = 100^o C, T_{ev} = 5^o C$)

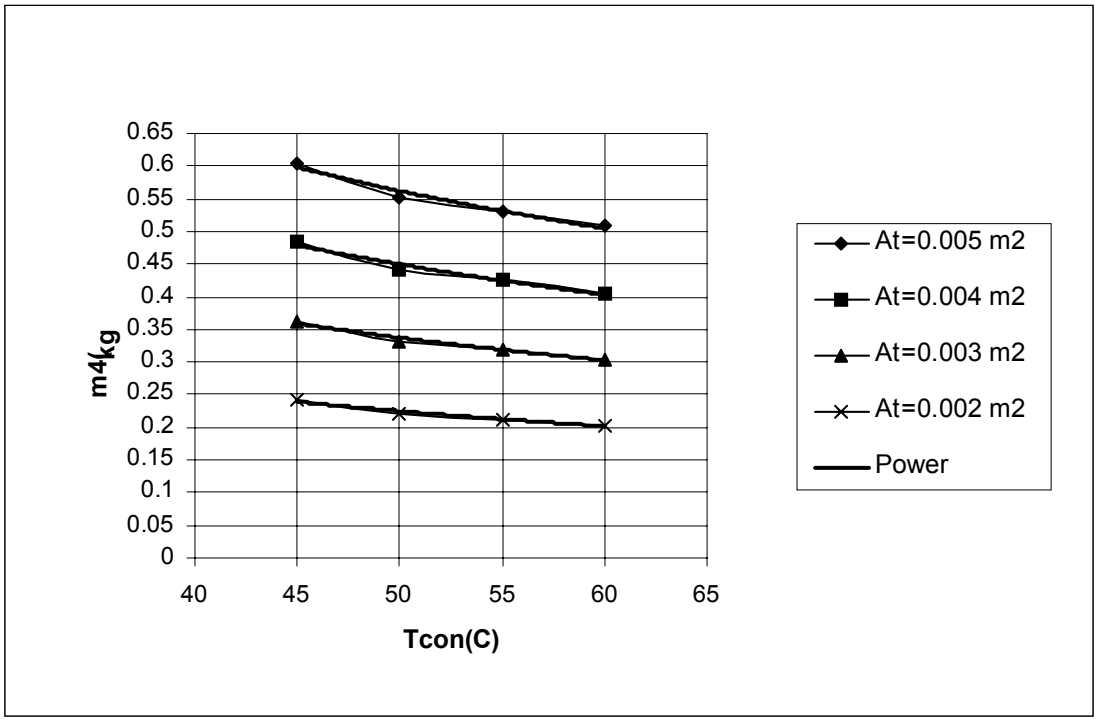

Fig (4-12) The curve fitting for the variation of the evaporator mass flow rate with condenser temperature at different throat areas. ($T_b = 100^o C, T_{ev} = 5^o C$)

4.2.2 Effect of the condenser temperature on the cooling coefficient of performance.

Fig (4-13) shows variation of cooling coefficient of performance (COP_c) of the system with condenser temperature at different throat areas for the indicated evaporator and boiler conditions.

It can be seen that the cooling coefficient of performance of the system remains constant at the different throat areas encountered in this study, but as the condensing temperature rises the cooling coefficient of performance drops and at condensing temperature range between 50 to 60^{o}C the rate of decrease becomes slower.

This behavior can be attributed to the decrease in refrigeration effect $(h_4 - h_7)$ at rising condensing temperature. Also figure (4-11) shows that the entrained vapor $(\dot{m}_4)$ flow rate is less at higher condensing temperature at constant boiling conditions.

Hence by referring to equation (3-44), it may be seen that the numerator of the equation are $(\dot{m}_4)$ and $(h_4 - h_7)$ which both are less at increasing condensing temperature.

The entrainment ratio for any throat area used seems to remain unchanged and this may explain that the (COP_c) for the different areas are at the same track. The results obtained are curve fitted and illustrated in figure (4-14) and obtained on the below equations.

$$COP_c = 0.0007 \times T_{con}{}^2 - 0.0766 \times T_{con} + 2.8901$$

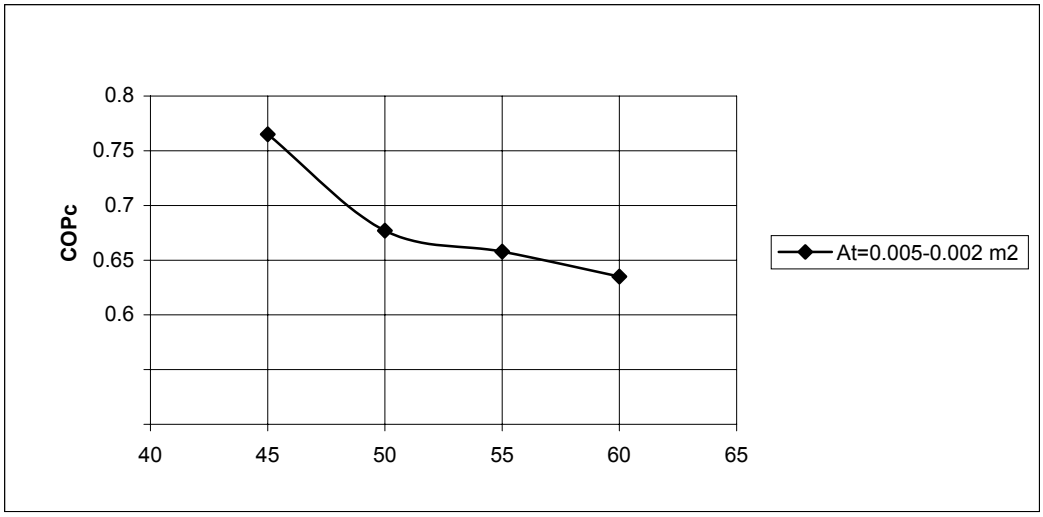

Fig (4-13) variation of cooling Coefficient of performance with condenser temperature at different throat areas ($T_b = 100^o C, T_{ev} = 5^o C$)

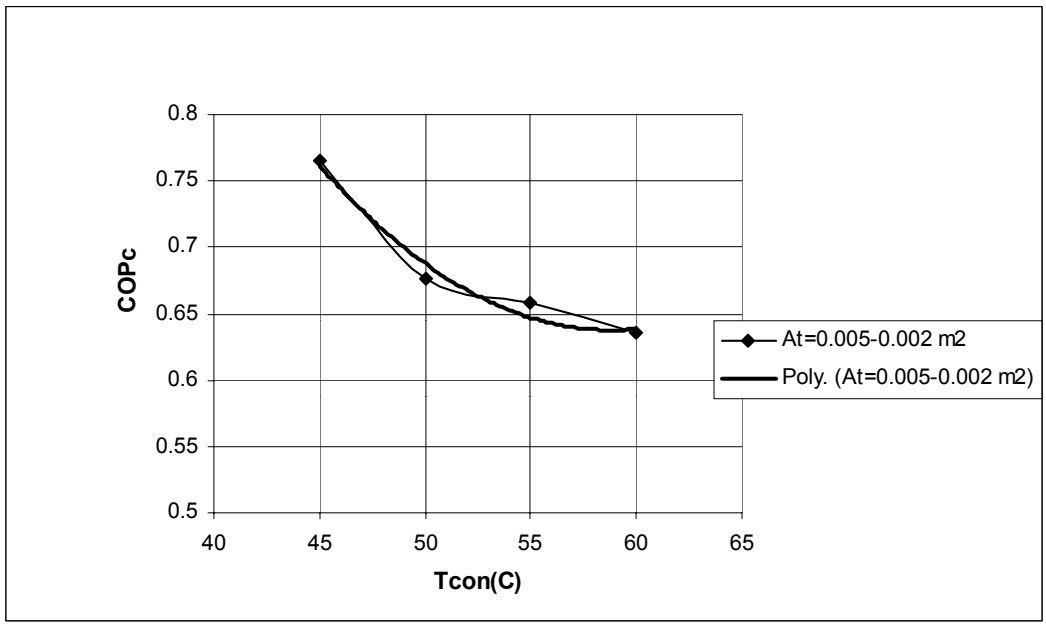

Fig (4-14) The curve fitting for the variation of cooling Coefficient of performance with condenser temperature at different throat areas ($T_b = 100^o C, T_{ev} = 5^o C$)

4.2.3 Effect of the condenser temperature on the heating Coefficient of performance.

Fig (4-15) shows variation of heating coefficient of performance (COP_h) of the system with condenser temperature at different throat areas at the conditions illustrated in the figure. It can be seen that the heating coefficient of performance of the system remains constant with different throat areas, and as condenser temperature increase the heating coefficient of performance (COP_h) of the system decrease and the rate of the decrease becomes less.

This behavior is due to the convergence between the condensing and boiler pressure and the change in latent of the vapor. As the condensing pressure rises at constant boiler pressure, the entrained mass flow rate and the latent heat of evaporation become less. Hence by inspecting equation (3-45), the numerator decreases as the condensing temperature becomes higher which results in less (COP_h). The results obtained are curve fitted and illustrated in figure (4-16) and obtained on the below equations.

$$COP_h = 2.1677 \times T_{con}^{-0.0048}$$

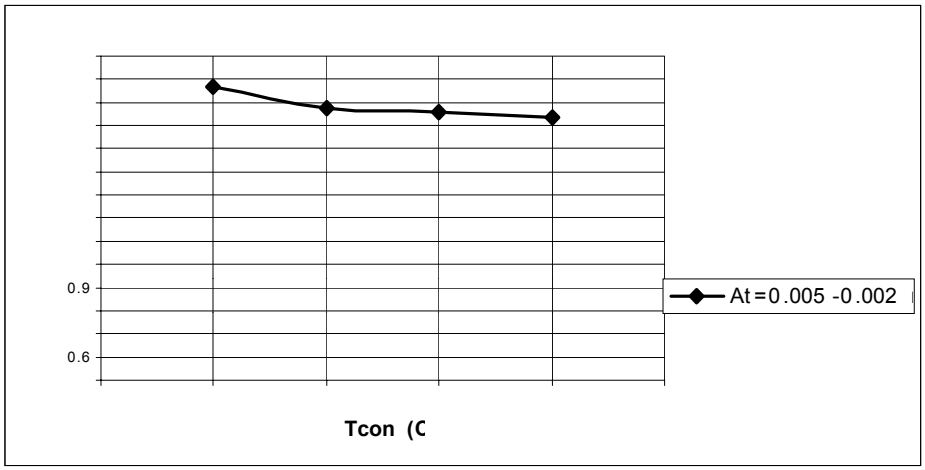

Fig (4-15) variation of heating Coefficient of performance with condenser temperature for at different throat areas ($T_b = 100^o C, T_{ev} = 5^o C$)

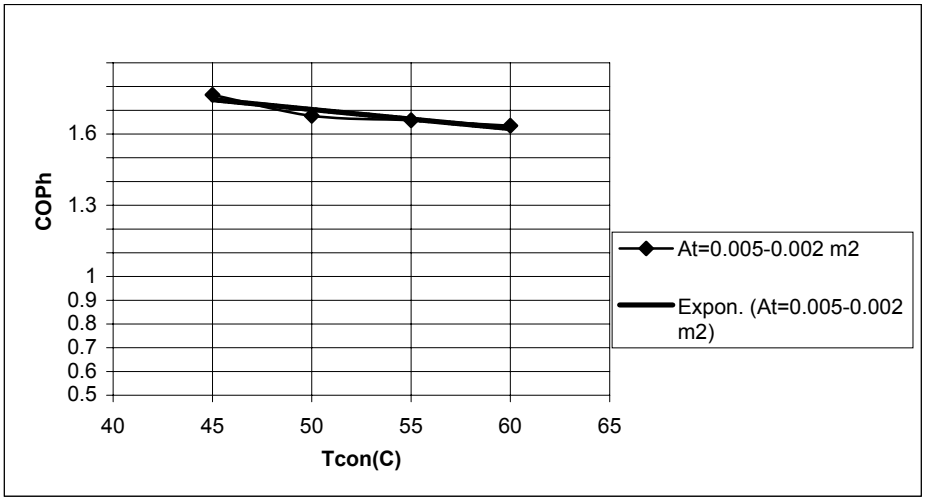

Fig (4-16) The curve fitting for the variation of heating Coefficient of performance with condenser temperature at different throat areas

$(T_b = 100^o C, T_{ev} = 5^o C)$

4.2.4 Effect of the condenser temperature on the system capacity.

Fig (4-17) shows variation of system capacity (Q) with condenser temperature ($Tcon$) at different throat areas at the conditions illustrated in the figure. It can be seen that the capacity decreased with condenser temperature rise and throat area increase, because of decreasing in the evaporator mass flow rate ($\dot{m}_4$) as discussed earlier. The results obtained are curve fitted and illustrated in figure (4-18) and obtained on the below equations.

$$Q = 14064 \times T_{con}^{-0.5899}$$

$$Q = 11426 \times T_{con}^{-0.5939}$$

$$Q = 8349.8 \times T_{con}^{-0.5872}$$

$$Q = 5710.8 \times T_{con}^{-0.5938}$$

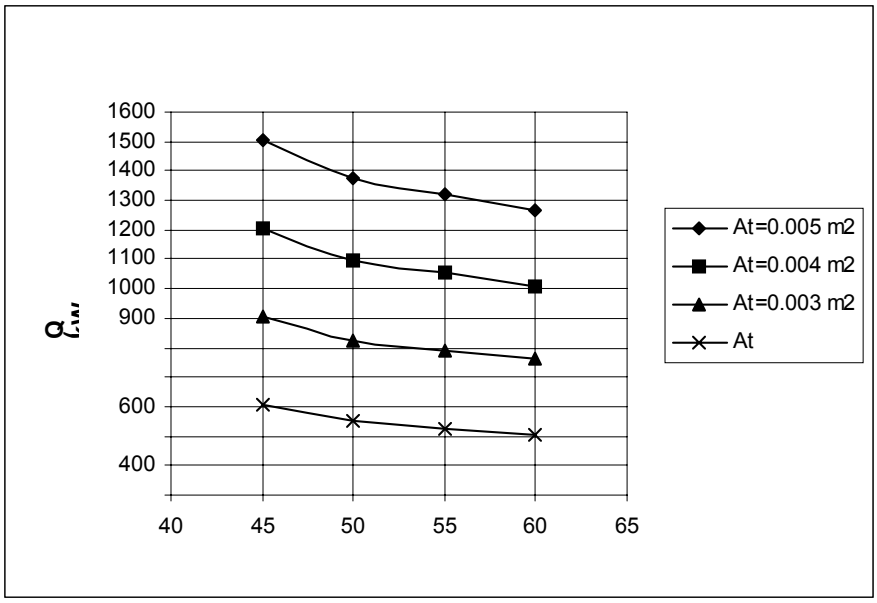

Fig (4-17) variation of system capacity with condenser temperature at different throat areas ($T_b = 100^o C, T_{ev} = 5^o C$)

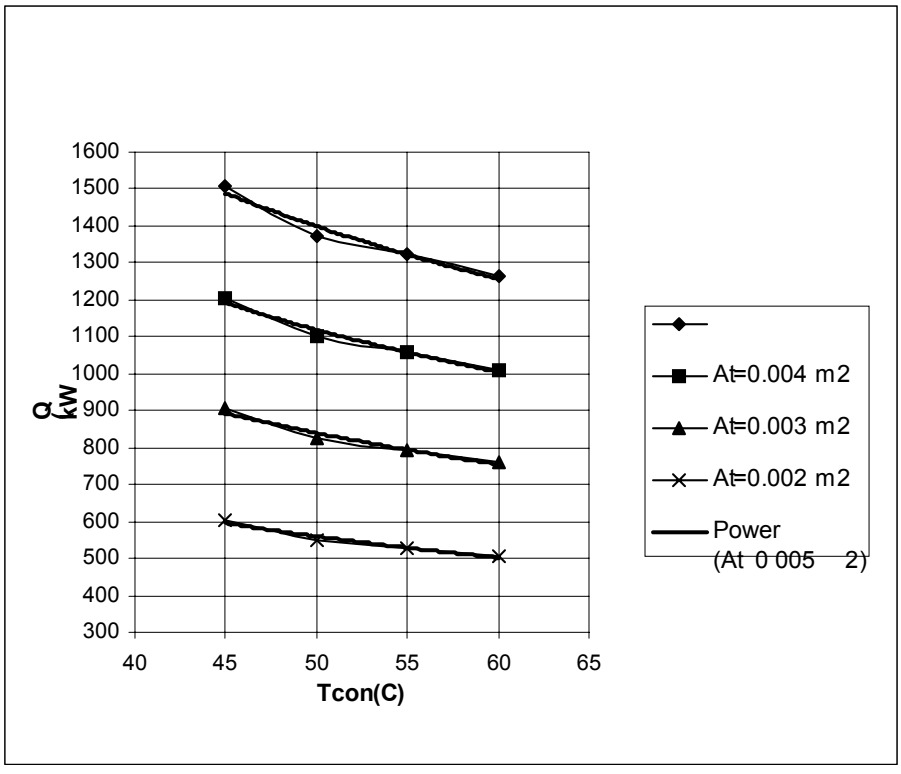

Fig (4-18) The curve fitting for the variation of system capacity with condenser temperature at different throat areas ($T_b = 100^o C, T_{ev} = 5^o C$)

4.3 The variation of the system characteristics with evaporator temperature for the variation throat areas.

4.3.1 Effect of the evaporator temperature on the evaporator flow rate.

Fig (4-19) shows variation of evaporator mass flow rate ($\dot{m}_4$) with evaporator temperature (T_{ev}) at different throat areas (A_t) at the conditions illustrated in the figure. It can be seen that the evaporator mass flow rate decrease with evaporator temperature rise and throat area increase, because as evaporator temperature increase the saturation pressure increase therefore the pressure variation between boiler and evaporator decrease, this lead to that the evaporator mass flow rate ($\dot{m}_4$) decreases.

The results obtained are curve fitted and illustrated in figure (4-20) and obtained on the below equations.

$$\dot{m}_4 = -0.0024T_e^{\,3} + 0.04T_e^{\,2} - 0.2517T_e + 1.1592$$

$$\dot{m}_4 = -0.0019T_e^{\,3} + 0.0314T_e^{\,2} - 0.1986T_e + 0.9231$$

$$\dot{m}_4 = -0.0014T_e^{\,3} + 0.024T_e^{\,2} - 0.1511T_e + 0.6955$$

$$\dot{m}_4 = -0.0009T_e^{\,3} + 0.0152T_e^{\,2} + 0.0966T_e + 0.4573$$

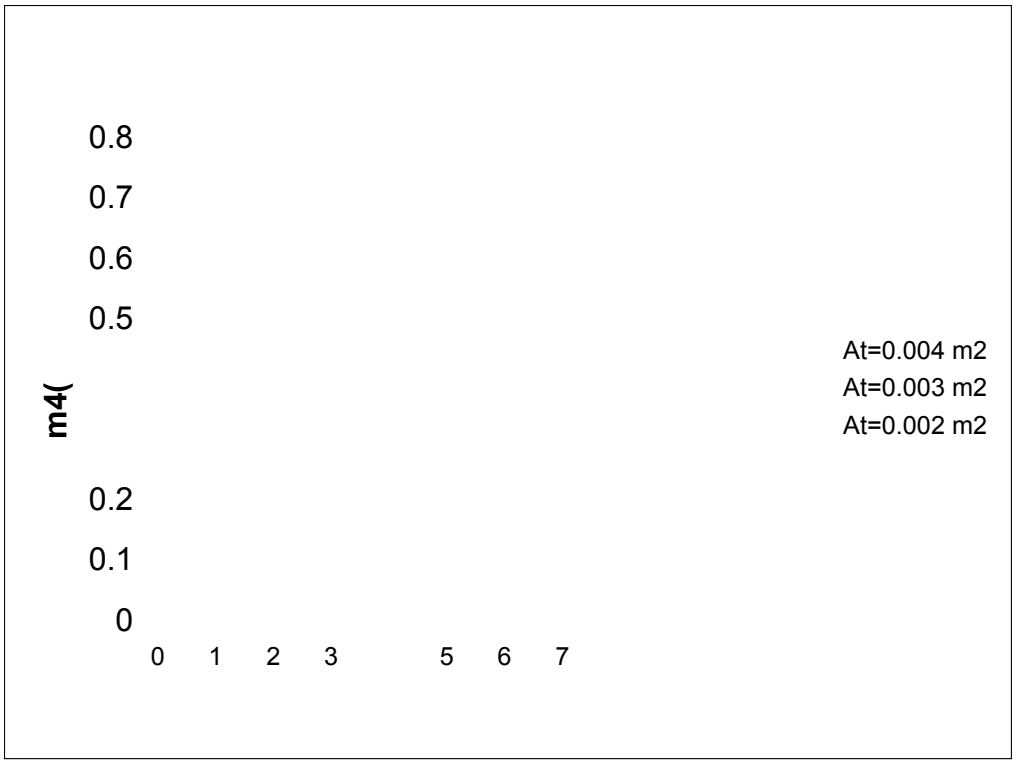

Fig (4-19) variation of evaporate mass flow rate with evaporator temperature for at different throat areas ($T_b = 100^o C, T_{con} = 45^o C$)

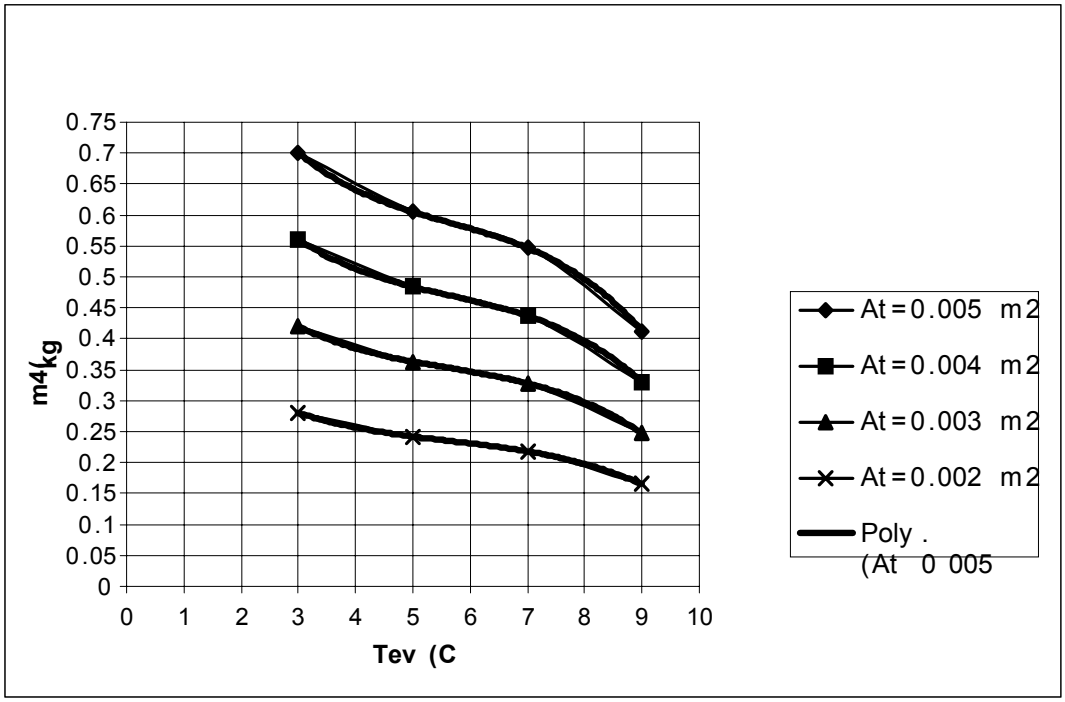

Fig (4-20) The curve fitting for the variation of the evaporate mass flow rate with evaporator temperature at different throat areas ($T_b = 100^o C, T_{con} = 45^o C$)

4.3.2 Effect of the evaporator temperature on the cooling Coefficient of performance.

Fig (4-21) shows variation of cooling coefficient of performance (COP_c) of the system with evaporator temperature at different throat areas at the conditions illustrated in the figure. It can be seen that the cooling coefficient of performance of the system remains constant with throat area variable, and as evaporator temperature increase the cooling coefficient of performance (COP_c) of the system decrease, because when the evaporator temperature increase the evaporator mass flow rate ($\dot{m}_4$) decreases, as discussed earlier, therefore the cooling coefficient of performance (COP_c) of the system decrease. The results obtained are curve fitted and illustrated in figure (4-22) and obtained on the below equation.

$$COP_c = 0.0014 \times T_{ev}{}^3 - 0.0315 \times T_{ev}{}^2 + 0.167 \times T_{ev} + 0.545$$

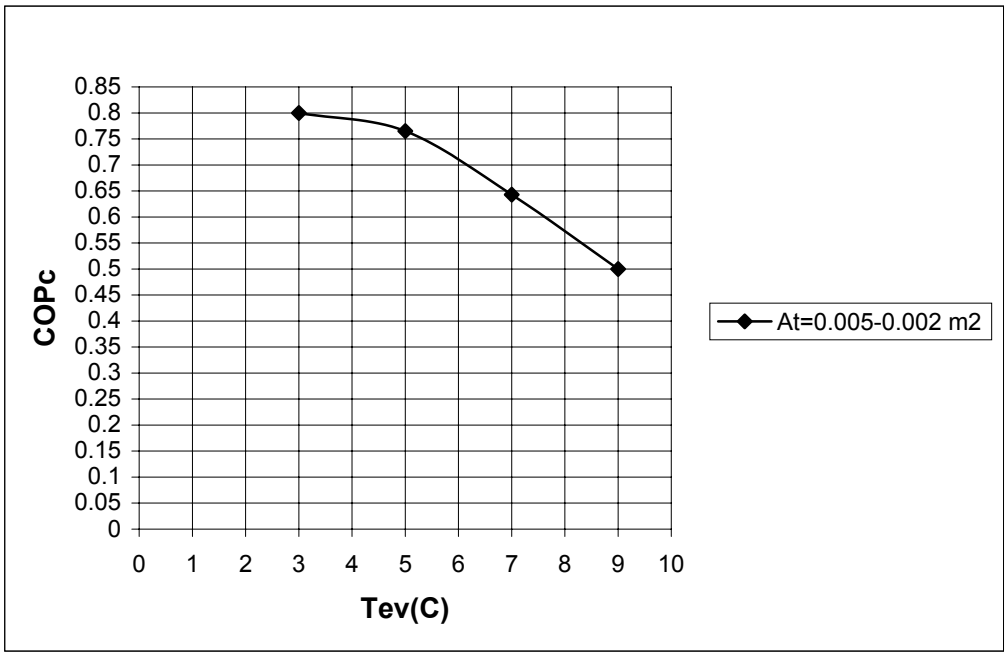

Fig (4-21) variation of cooling Coefficient of performance with evaporator temperature at different throat areas ($T_b = 100^o C, T_{con} = 45^o C$)

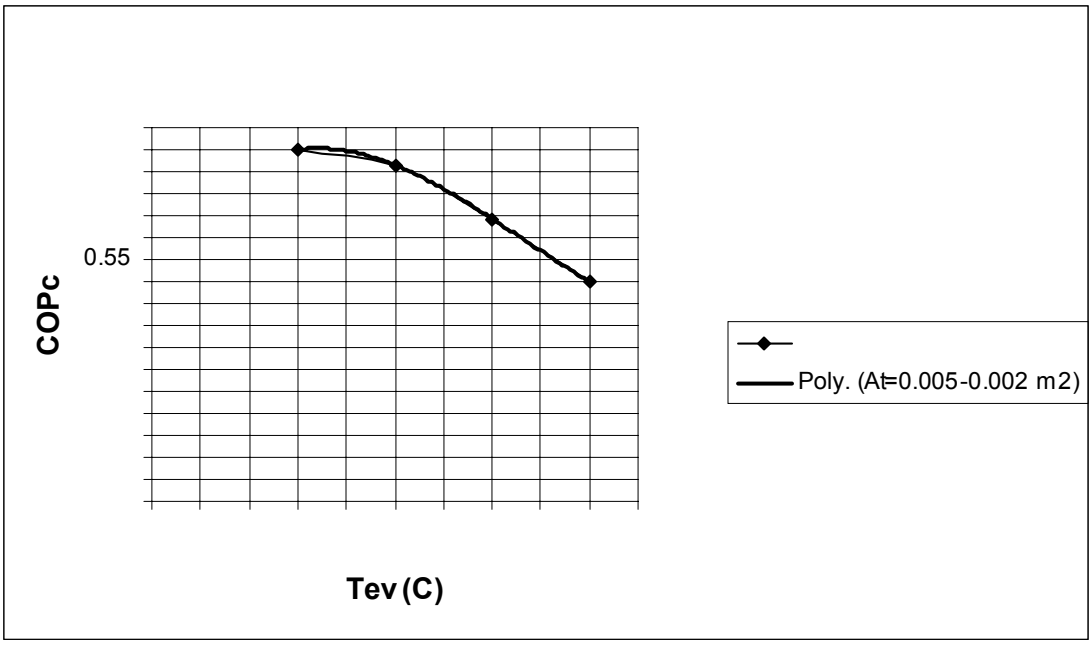

Fig (4-22) The curve fitting for the variation of cooling Coefficient of performance with evaporator temperature at different throat areas

$(T_b = 100^o C, T_{con} = 45^o C)$

4.4 Comparison of the Coefficients of performance between the Steam jet refrigeration system and the Absorption system with condenser temperature.

Fig (4-23) shows variation of cooling coefficient of performance (COP_c) of the two systems with condenser temperature at a given evaporator temperature (5^oC). It can be seen that the cooling coefficient of performance of the two system decreases with condenser temperature rise, but the cooling coefficient of performance of the steam jet refrigeration system remains greater than the absorption system at the same capacity and input characteristic. This may be attributed to the fact that in Absorption refrigeration heat is rejected in two locations i.e. in the condenser and absorber, while in Steam jet heat is rejected in condenser only. The reason for this behavior of the steam jet as discussed in section (4.2.2).

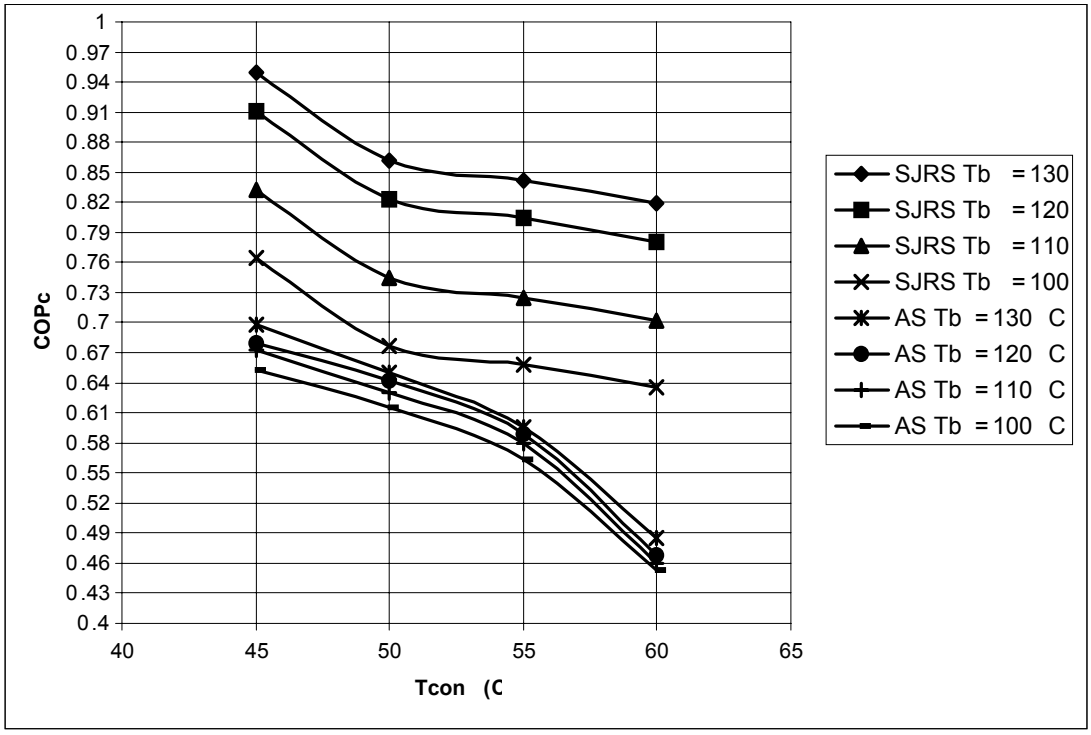

Fig (4-23) the cooling Coefficient of performance for the steam jet refrigeration system and the absorption system with the condenser temperature.

4.5 Comparison of the Coefficients of performance between the Steam jet refrigeration system and the Absorption system with evaporator temperature.

Fig (4-24) shows variation of cooling coefficient of performance (COP_c) of the two systems with evaporator temperature. It can be seen that the cooling coefficient of performance of the steam jet refrigeration system decreases with evaporator temperature rise, as discussed in section (4.3.2), but the cooling coefficient of performance of the absorption system increases at the same capacity and input characteristic. Thus because the evaporator mass flow rate in the steam jet refrigeration system decrease at evaporator temperature rise therefore the (COP_c) of the system decrease.

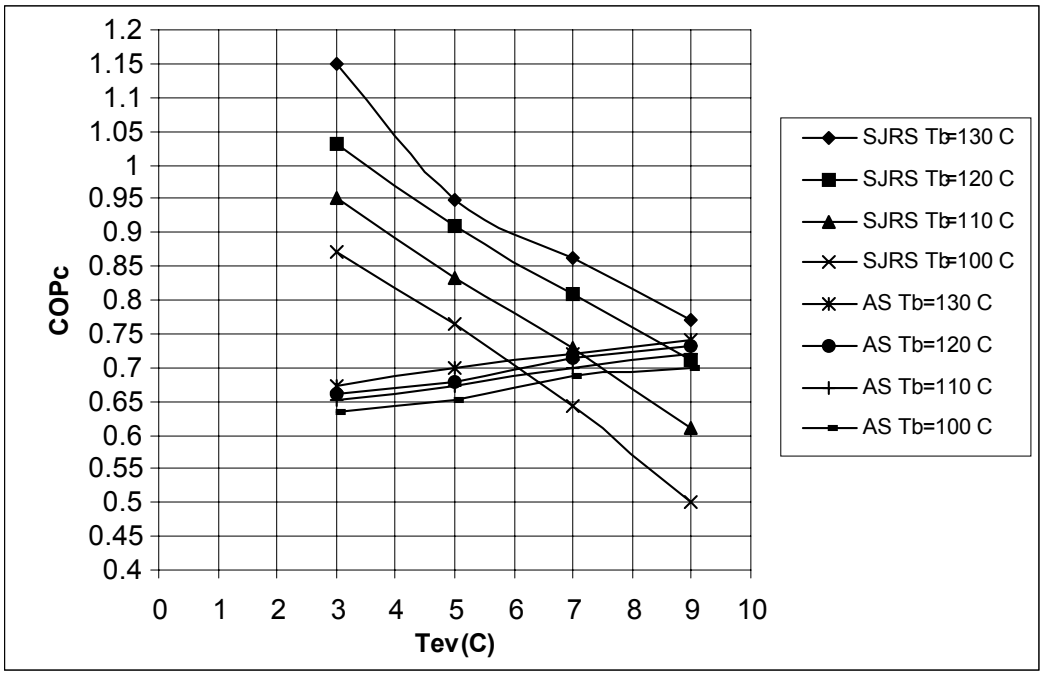

Fig (4-24) the cooling Coefficient of performance for the steam jet refrigeration system and the absorption system with the evaporator temperature.

Chapter five

Conclusions and Recommendations for future work

5.1 Conclusions: -

The following has been concluded from the case studies done for the steam jet refrigeration system analysis:

1. For a given ejector throat area, and constant condensing and evaporating temperature, The secondary vapor mass flow rate was found to increase with increasing boiler temperature, thus giving rise to cooling capacity.
2. The secondary mass vapor flow rate was found to increase with increasing ejector throat area at constant boiler temperature, condensing and evaporating temperatures.
3. For a given ejector throat area and constant boiler and evaporating temperatures, the secondary vapor mass flow rate was found to decrease with increasing condensing temperature, thus dropping the cooling capacity.
4. The larger throat area is the higher secondary vapor mass flow rate and higher system capacity at a given set of conditions.
5. At a given ejector throat area and constant condensing and boiler temperatures, the secondary vapor mass flow rate was found to decrease with increasing evaporating temperature, thus resulting in drop of cooling capacity.
6. The cooling coefficient of performance of Steam jet and Absorption system was found to decrease with condenser temperature rise, but the

cooling coefficient of performance of the former system is larger than the later one. Both at a given evaporator temperature.

7. The cooling coefficient of performance of the steam jet refrigeration system is found to decrease with evaporator temperature rise, but the cooling coefficient of performance of the absorption system is found to increase.
8. At boiler temperature 130^{o}C the C.O.P. of the steam jet is grater than the Absorption system at evaporator temperature range (3-9^{o}C).
9. The C.O.P. of the steam jet refrigeration was found to be higher than that of Absorption system at boiler temperatures exceeding 120^{o}C. Below 120^{o}C, the later system C.O.P. becomes larger than that the former system at evaporating temperature exceeding 7^{o}C.

5.2 Recommendations for future work: -

1. Two ejectors, in series, may be used to increase the cooling capacity of the system.
2. A study of the performance of the system under transit conditions is also required.
3. To apply the present system design for a different capacity, new set of calculation should be made to obtain the proper parameters for the best performance, depending on the equations as a result from curves fitting shown previous.